702

ISSN 0136-3549
0134-3823

TALLINNA TEHNIKAÜLIKOOLI

TOIMETISED

ТРУДЫ ТАЛЛИННСКОГО ТЕХНИЧЕСКОГО УНИВЕРСИТЕТА

TRANSACTIONS OF TALLINN TECHNICAL UNIVERSITY

ANALYSIS AND SYNTHESIS
OF COMPLICATED SYSTEMS
AND CIRCUITS WITH THE AID
OF COMPUTERS

TALLINN 1989

702

ALUSTATUD 1937

TALLINNA TEHNIKAÜLIKOOLI TOIMETISED

TRANSACTIONS OF TALLINN TECHNICAL UNIVERSITY

ТРУДЫ ТАЛЛИННСКОГО ТЕХНИЧЕСКОГО УНИВЕРСИТЕТА

УДК 681.5

ANALYSIS AND SYNTHESIS OF COMPLICATED SYSTEMS AND CIRCUITS WITH THE AID OF COMPUTERS

Electrical Engineering and Automatics XXXVIII

TALLINN 1989

Contents

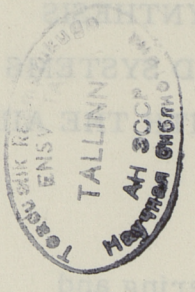

No 702

TALLINNA TEHNIKAÜLIKOOLI TOIMETISED
TRANSACTIONS OF TALLINN TECHNICAL UNIVERSITY

UDC 681.51

A. Kull

A FORMAL MODEL FOR AUTOMATED TECHNOLOGICAL SYSTEM

Abstract

In this paper a formal model is proposed to describe automated technological systems. Automated technological system is treated as a discrete event dynamic system. The proposed model consists of concurrent processes which are connected with unidirectional channels. The processes are represented as extended state machines. The system model is a universal tool for real-time control system design and its creation is fairly simple.

1. Introduction

Process control system (PCS) is a man–machine system dedicated to control a technological process optimally in the sense of the given economical or technological criterion. PCS is a control system with regard to technological process as a control plant and together they form a new man–machine system which we call an automated technological system (ATS). To design a PCS we do not need only a mathematical model of technological process but we must also be able to model the behavior of the entire ATS.

Traditionally, process models describe the relations between process variables using ordinary or partial differential equations or transfer matrices. The models are not suitable for ATS, because firstly, the models' complexity rises rapidly, and secondly, it is useless to describe quantitatively all the changes of process states. Often it is necessary to describe only qualitative changes.

ATS is a complex man–machine system that consists of

different elements. ATS elements are connected together by material, energy, and information flows. Each ATS element is a functionally independent unit of the ATS. Its state exerts influence on the behaviour of entire ATS or is supervised by operator. At any time each ATS element stays in one possible discrete state. ATS element discrete state describes its qualitatively different working regimes, for example "working", "not working", "breakdown". ATS elements behaviour is described by a discrete state transition graph, where the nodes represent discrete states and the arcs represent admissible transitions between these states. Changes of discrete states are caused by events. Events are changes of states in other elements or in environment. Therefore we can treat ATS as discrete event dynamic system (DEDS), which is discretisized by the time of the events' occurrence.

DEDS can be described by Petri nets [1]. Petri nets are one of the best known formalism for dealing with real-time DEDS [2]. Petri nets have been found useful for representing concurrency and causal dependence of events. Another formalism for dealing with DEDS is a net of state machines [3, 4]. Interesting results in modelling DEDS have been achieved by J.S. Ostroff with his ESM (Extended State Machine) formalism [5]. ESM is an extension of state machines, which has the added features of time bounded events as well as explicit mention of both the states and events.

In this paper we discuss discrete event model (DEM) as a universal tool to model ATS. To develop a DEM we improve Ostroff's ESM so that

1) we can use our model to design and develop real-time control systems,

2) we can create the control system without programming in the traditional manner, but using descriptions.

2. Modelling ATS

DEM consists of many concurrent processes [1]. Each process models an ATS element. To model causal dependence between ATS elements, we connect processes by unidirectional channels. Channels are used to transfer messages between

[1] Here and further we use the term "process" in the sense of computer science, but not as a technological process.

processes. Process discrete state expresses discrete state of ATS element at a given moment of time. Transition from one discrete state to another is caused by events in other processes, in environment or in process himself.

3. DEM

DEM M consists of concurrent processes M_i.

$$M = M_1 \,||\, M_2 \,||\, \ldots \,||\, M_n$$

Process M_i is a 4-tuple

$$M_i = (X_i, Y_i, C_i, T_i), \text{ where}$$

X_i - discrete state variable;

Y_i - set of process variables;

C_i - set of communication channels;

T_i - set of rules, which define the order of discrete state changes.

Process state is defined by values of discrete state variable and process variables.
At any time a process has a discrete state. X_i expresses the current discrete state of process M_i. Type of X_i is type (X_i). It means that its values are from set type (X_i). This set has finite number of elements. Every process may have many process variables. Each variable y_{ij} in Y_i has type type (Y_{ij}). This type is a set with infinite number of elements.

A message passing between processes proceeds along the communication channels.

Rules T_i are discussed in 3.4.

3.1. Events

The event is a change of the process state. It is an essential concept of DEM. The events activate processes. Without events the processes are passive. Processes activate if in their surroundings an event occurs that may cause process state change.

There are four kinds of events:

1) changing of process variable's value,

2) message sending,

3) message receiving,

4) passing an interval of time.

3.2. Communication

Synchronisation and communication between processes occur by message passing. Message sending and receiving proceed by communication operators.

Message sending proceeds using operator Channel! Msg, where

Channel - name of the communication channel,

Msg - message.

Message may be any expression including constants, process variables and discrete state variable. Each message has a type type (Msg). Each channel has a type type (Channel). Type of channel determines type of message that can be sent through this channel. It means that it must be guaranteed that type(Channel)=type(Msg).

Message receiving proceeds using operator Channel?Pvar, where

Channel - name of the communication channel from which process waits a message.

Pvar - process variable.

Message from channel Channel will be assigned to process variable Pvar. It must be guaranteed that type(Channel) =type(Pvar).

Message receiving is an asynchronous process. It means that message sending process continues its work after sending a message. Message waiting process will be stopped until the message arrives.

3.3. Timer

The Timer or model clock is a process, too. The Timer allows to simulate spontaneous events in the environment. The Timer may be connected with each process. From the point of view of other processes the Timer is a server offering the following services:

1) activating a process after fixed interval of time,

2) activating a process repeatedly after fixed interval of time.

To use these services a process sends to Timer a message of the following format: (service, parameter). According to the above list there are two types of services: wakeupAfter or wakeupAfterEach with a parameter interval. The Timer service reduces to sending a message wakeup to a customer-process at the proper time.

3.4. Change of discrete states

Changes of process discrete states are determined by a set of rules T_i. Each element t_{ij} in T_i is 4-tuple

(x_s, TC, OP, x_d), where

x_s - source discrete state,

x_d - destination discrete state,

TC - guard that must be satisfied to enable a state change from x_s to x_d,

OP - operation that will be performed before states change.

Guard checks if there was such an event that causes a change of discrete state.

4. Example

Let us consider a simple example - a process control system that controls the gate on a railway crossing. The gate must be down if the train is in the danger zone and it must be up if the train is in the safe zone. We model this system using DEM. Our model consists of three processes - Train, Gate, GateController and Timer (Fig. 1). The process Train models the train motion. Let there be a circular railway and the train is moving with constant speed. With respect to the railway crossing the train has two possible discrete states - "dangerous" and "safe". To initialize our model functioning we assume an additional discrete state "init". Let us assume also that the train stays in the discrete state "dangerous" during dangerousTime and in the discrete state "safe" during safeTime. The train dynamic behaviour is modelled using Timer services.

The channel m connects the process Train with the

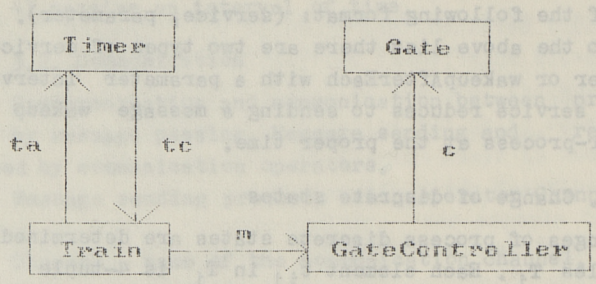

Fig. 1. Model of railway crossing control system.

process GateController. If in the process Train a discrete state change occurs, a message about the discrete state of the Train is transferred through the channel m to the Gate Controller. If it is necessary to change the Gate position, the GateController sends a message to the Gate through the channel c. The process Train communicates with the Timer via channels ta and tc. The channel ta is used to transfer requests for the Timer services and the channel tc - to transfer the Timer messages.

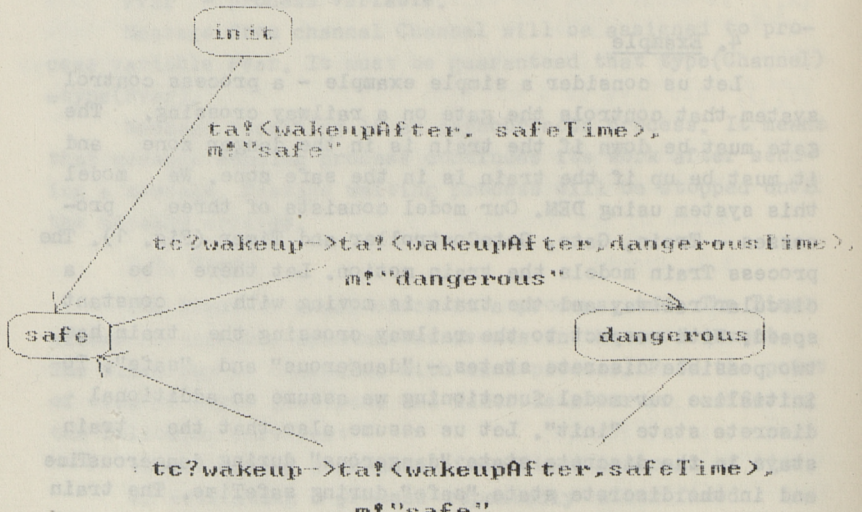

Fig. 2. Train state transistion graph.

The process Train discrete state transition graph is presented in Fig. 2. At the initial moment of time the Train current discrete state is "init". The state transition from "init" to "safe" has a guard which is always true. Therefore the operations will be executed and the Train current discrete state changes to "safe". Operations performed during this execution are sending the messages ta! (wakeupAfter, safeTime) (with this message the Train says to the Timer: "wake me up again after safeTime", and m! "safe" (to send a message with new current discrete state into channel m). The Train waits in the current discrete state "safe" until the Timer wakes it up again. The Timer wakes the Train up sending it the message "wakeup". The process Train performs its operations according to the state transition graph and the Train current discrete state changes to "dangerous".

The process GateController discrete state transition graph is presented in Fig. 3. If the GateController current discrete state is "up" and it receives a message that the train is in a dangerous zone, it sends a message through the channel c to the Gate with the command to shut the gate. If the GateController current state is "down" and it receives a message that the train is safe, it sends to the Gate a message with a command to open the gate.

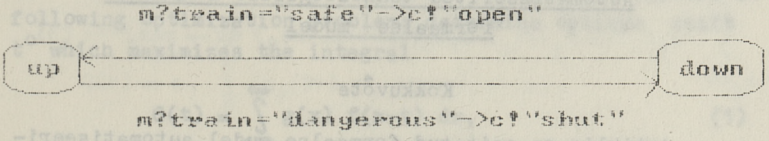

Fig. 3. GateController state transition graph.

5. Conclusion

DEM is quite a universal tool to develop real-time control systems. We can develop a control system using simple descriptions. Therefore we can declare that DEM is a good knowledge representation scheme for real-time systems. DEM is the next step to knowledge-based real-time systems.

6. References

1. Peterson J.L. Petri Net Theory and the Modelling of Systems. Prentice Hall, Englewood Cliffs, N.J., 1981.

2. Leveson N.G., Stolzy J.L. Safety analysis using Petri nets // IEEE Transactions on Software Engineering. SE-13(3): 386-397.

3. Auernheimer, B., Kemmerer R.A. Rt-aslan: a specification language for real-time systems //IEEE Transactions on Software Engineering. SE-12(9): 879-889. Sept. 1986.

4. Zave, P. An operational approach to requirements specification for embedded systems //IEEE Transactions on Software Engineering, SE-8(3): 250-269, May 1982.

5. Ostroff J.S. Modular reasoning in the ESM/RTTL framework for real-time systems. Technical Report No CS-88--03. Department of Computer Science, York University, North York, Ontario, 1988.

A. Kull

Automatiseeritud tehnoloogilise kompleksi formaalne mudel

Kokkuvõte

Artiklis on esitatud formaalne mudel automatiseeritud tehnoloogilise kompleksi kirjeldamiseks. Automatiseeritud tehnoloogilist kompleksi vaadeldakse kui diskreetset sündmuslikku dünaamilist süsteemi. Esitatud mudel koosneb paralleelselt töötavatest protsessidest, mis on ühendatud omavahel ühesuunaliste kanalitega. Protsessid kujutavad endast laiendatud lõplikke automaate. Artiklis esitatud formalism on küllalt universaalne mitmesuguste reaalaja juhtimissüsteemide mudelite loomiseks.

No 702

TALLINNA TEHNIKAÜLIKOOLI TOIMETISED
TRANSACTIONS OF TALLINN TECHNICAL UNIVERSITY

UDC 681.514

A. Kiitam

AN APPROXIMATE SOLUTION FOR THE ONE-DIMENSIONAL OPTIMUM SHIFT PROBLEM WITH GAUSSIAN UTILITY FUNCTION AND TRUNCATED GAUSSIAN DISTRIBUTION

Abstract

An equation is derived for the solution of one-dimensional optimum shift problem with Gaussian utility function and truncated Gaussian distribution. Two approximate solutions for this equation and their tangent-based improvement are considered.

1. The Problem

The one-dimensional optimum shift problem appears as following optimization problem: determine optimum shift t^{o} which maximizes the integral

$$G(t) = \int_{-\infty}^{\infty} g(x)\, f(x-t)\, dx, \qquad (1)$$

where $g(x)$ is a utility function and $f(x)$ is a distribution density for stochastic variable x. Such problem arises in various technological activities, e.g. in design centering (Director and Hachtel, 1977) and in parametric correction (Abramov, Bernatski and Zdor, 1982). Different situations lead to different specific forms of $g(x)$. For instance, for yield maximization problem we have $g(x)=1$ within tolerance interval (e_x, l_x) and $G(t)$ is the yield as probability $P(e_x \leqslant x \leqslant l_x)$. In this paper we consider an optimum shift problem with Gaussian utility function $\exp(-x^2)$ and truncated Gaussian distribution. Such problem arises, for in-

stance, as asymptotic case of the optimum shift problem for linear stratified compensation systems (Kiitam and Saks, 1987) with Gaussian noise and yield maximization criterion.

Let $n_o(x)$ be the normalized Gaussian distribution density and $N_o(x)$ the corresponding distribution function, i.e: $n_o(x) = (2\pi)^{-1/2}\exp(-x^2/2)$. $N_o(x) = \int_{-\infty}^{x} n_o(y)\,dy$. The optimization problem considered is represented as (1) with

$$g(x) = c_g n_o((x-m_g)/s_g),$$

$$f(x-t) = \begin{cases} c_f n_o((x-t-m_f)/s_f), & e_x+t \le x \le l_x+t \\ 0, & x < e_x+t, \quad x > l_x+t \end{cases} \qquad (2)$$

where c_g, m_g, s_g, c_f, m_f, s_f are some constants (c_g, c_f, s_g, $s_f > 0$) and

$$c_f = (s_f(N_o((l_x-m_f)/s_f) - N_o((e_x-m_f)/s_f)))^{-1}.$$

Thus, the integral to be maximized is expressed as

$$\int_{e_x+t}^{l_x+t} c_g n_o((x-m_g)/s_g)\; c_f n_o((x-t-m_f)/s_f)\,dx \to \max_t. \qquad (3)$$

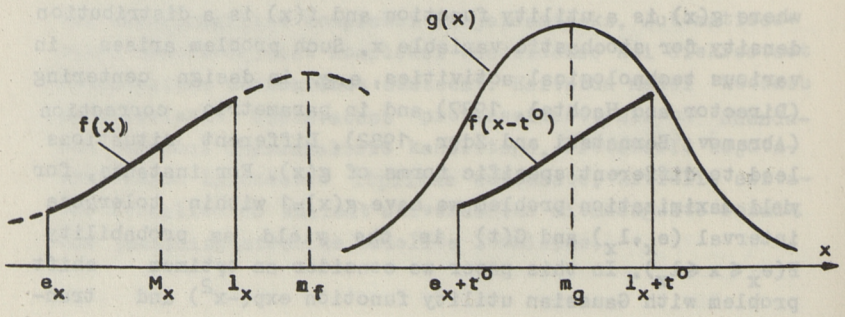

Fig. 1. Optimum shift problem.

2. Some Transformations

Denote $w=(x-t-m_f)/s_f$, then $(x-m_g)/s_g=(w-((m_g-m_f-t)/sf))/(s_g/s_f)$; thus we obtain the problem

$$Q(u) = c_1 \int_e^l n_0((w-u)/A)\, n_0(w)\, dw \to \max_u, \qquad (4)$$

where

$$e = (e_x-m_f)/s_f,$$

$$l = (l_x-m_f)/s_f,$$

$$u = (m_g-m_f-t)/s_f,$$

$$A = s_g/s_f,$$

$$c_1 = c_g c_f s_f > 0.$$

In (4) we have

$$n_0((w-u)/A)\, n_0(w) = n_0(Bv)\, n_0((w-v)/s,$$

where

$$v = u/(A^2+1),$$

$$s = A(A^2+1)^{-1/2},$$

$$B = (A^2+1)^{1/2}.$$

Thus

$$Q(v) = c_1 \int_e^l n_0(Bv)\, n_0((w-v)/s)\, dw =$$

$$= c_1 s\, n_0(Bv)\, (N_0((l-v)/s)-N_0((e-v)/s)),\ c_1 s > 0.$$

Correspondingly, if v^0 is the solution for the problem

$$q(v) = n_0(Bv)\, (N_0((l-v)/s)-N_0((e-v)/s)) \to \max_v,$$

then the solution for initial problem (3) is expressed through $u^0=v^0(A^2+1)$ with $t^0=m_g-m_f-s_f u^0$.

From $dq(v)/dv=0$ we get the equation

$$-B^2 v\, n_0(Bv)\, (N_0((l-v)/s) - N_0((e-v)/s) +$$
$$+ n_0(Bv)\, (n_0((e-v)/s) - n_0((l-v)/s))/s) = 0.$$

As $n_0(Bv) \neq 0$, we get for v° the equation

$$B^2 sv = \frac{n_0((e-v)/s) - n_0((l-v)/s)}{N_0((l-v)/s) - N_0((e-v)/s)}.$$

Denote

$$z = (e-v)/s,$$

$$d = (l-e)/s,$$

$$r(z,d) = \frac{n_0(z) - n_0(z+d)}{N_0(z+d) - N_0(z)}$$

with $v = -sz+e$. Correspondingly we get the equation

$$-B^2 s^2 z + B^2 se = r(z,d).$$

Thus, to find the optimum shift we have to solve the equation

$$-az + b = r(z,d) = \frac{n_0(z) - n_0(z+d)}{N_0(z+d) - N_0(z)}, \quad d, a > 0, \tag{5}$$

where

$$a = s_g^2/s_f^2,$$

$$b = (a(a+1))^{1/2} e,$$

$$d = (l-e)/s,$$

$$e = (e_x - m_f)/s_f,$$

$$l = (l_x - m_f)/s_f.$$

The solution z° for (5) provides the optimum shift t° by

$$t^\circ = m_g - m_f + T, \tag{6}$$

$$T = (1+a)^{1/2} s_g z^\circ - (1+a) s_f e. \tag{7}$$

3. Approximate Solution

As we can see from Fig. 2, $r(z,d)$ is monotonous increasing function with asymptotes

$$\lim_{z \to \infty} r(z,d) = z,$$

$$\lim_{d \to 0} r(z,d) = z,$$

$$\lim_{d \to \infty} r(z,d) = n_0(z)/(1-N_0(z)) = n_0(-z)/N_0(-z).$$

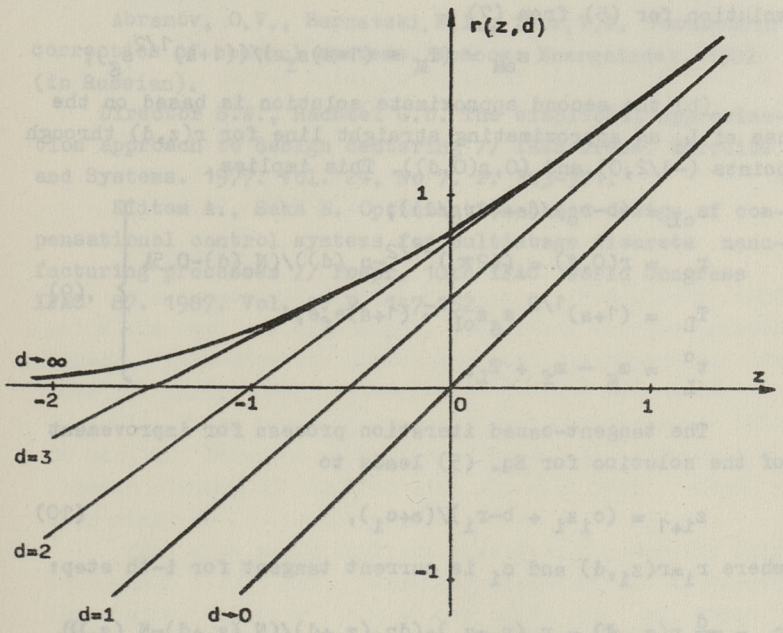

Fig. 2. Function r(z, d).

Thus, $r(z,d)$ changes between bisector $r(z,d)=z$ and reciprocal of Mills' ratio $(1-N_0(z))/n_0(z)$. For most values of z and d, especially if d is small ($d<3$) or z is large, $r(z,d)$ is close to linear function with derivative about

+1. Correspondingly, tangent-based iterative algorithms are effective to solve Eq. (5).

To find the approximate value of optimum shift t^o, which also implies an initial solution for Eq. (5) iteration process, two possibilities seem to be reasonable:

(a) the first one is based on the use of utility function $g(x)=-(x-m_g)^2$. This yields the shift value which corresponds to the mean M_x of distribution f(x), i.e.

$$T_M = s_f M_x = s_f(n_o(e)-n_o(1))/(N_o(1)-N_o(e)) \qquad (8)$$

with $t^o_M=m_g-m_f+T_M$ from (6) and with corresponding initial solution for (5) from (7)

$$z_{oM} = (T_M + (1+a)s_f e)/((1+a)^{1/2}s_g);$$

(b) the second approximate solution is based on the use of L_o as approximating straight line for r(z,d) through points (-d/2,0) and (0,r(0,d)). This implies

$$\left.\begin{aligned} z_{oL} &= (b-r_o)/(a+(2r_o/d)),\\ r_o &= r(0,d) = ((2\pi)^{-1/2}-n_o(d))/(N_o(d)-0.5),\\ T_L &= (1+a)^{1/2}\, s_g z_{oL} - (1+a)s_f e,\\ t^o_L &= m_g - m_f + T_L. \end{aligned}\right\} \qquad (9)$$

The tangent-based iteration process for improvement of the solution for Eq. (5) leads to

$$z_{i+1} = (c_i z_i + b - r_i)/(a+c_i), \qquad (10)$$

where $r_i=r(z_i,d)$ and c_i is current tangent for i-th step:

$$c_i = \frac{d}{dz} r(z_i,d) = r_i(r_i-z_i)+(dn_o(z_i+d)/(N_o(z_i+d)-N_o(z_i))). \qquad (11)$$

For small values of d ($d<3$) it is possible to simplify (11) by the use of approximating constant tangent which corresponds to line L_o; then $c_i=c_o=2r_o/d$.

Some numerical tests using above formulas were performed mainly for the case $a=1$ ($s_g=s_f$). The results permit to conclude that:

(1) the mean-based approximate solution (8) is "in average" better than L_0-based solution (9). However, L_0-solution is sometimes better for trapezoid-like f(x) . The error $h = |z^0 - z_{oM}|$ decreases if d decreases (for a=1 the error is about $h < 10^{-1}$, and $h < 10^{-2}$ if $d < 1.2$, $h < 10^{-3}$ if $d < 0.6$);

(2) the convergence of iteration process (10) is rapid. Each iteration usually leads to approximately one order of values improvement for the solution. Thus, in practice only few (about 1...4) iterations are usually needed to obtain sufficiently accurate solution.

References

Abramov, O.V., Bernatski, F.I., Zdor, V.V. Parametric correction of control systems. Moscow: Energoizdat, 1982 (in Russian).

Director S.W., Hachtel G.D. The simplicial approximation approach to design centering // IEEE Trans. Circuits and Systems. 1977. Vol. 24, No 7. P. 363-371.

Kiitam A., Saks E. Optimization-based design of compensational control systems for multistage discrete manufacturing processes // Prepr. 10th IFAC World Congress IFAC' 87. 1987. Vol. 4. P. 147-152.

A. Kiitam

Ligikaudne lahendus ühemõõtmelisele optimaalnihke ülesandele Gaussi kasulikkusfunktsiooni ja lõigatud Gaussi jaotuse korral

Kokkuvõte

On tuletatud võrrand ühemõõtmelise optimaalnihke ülesande lahendamiseks Gaussi kasulikkusfunktsiooni ja lõigatud Gaussi jaotuse korral. Vaadeldakse selle võrrandi kaht ligikaudset lahendit ja nende parandamist puutuja abil.

No 702

TALLINNA TEHNIKAÜLIKOOLI TOIMETISED
TRANSACTIONS OF TALLINN TECHNICAL UNIVERSITY

UDC 681.514

A. Bachverk

CALCULATION OF STOCHASTIC CHARACTERISTICS OF DIGITAL-TO-ANALOG CONVERTER SINE OUTPUT SIGNAL SPECTRUM

Abstract

Sketches are given of two possibilities of sine signal generation as discrete periodic signal. In real situation this signal has a random deviation from a given form. A simulation experiment is to be performed for calculation of stochastic characteristics of discrete periodic signal spectrum.

Introduction

The functional digital-to-analog converters (FDAC) which are used for sine signal generation in same measuring scheme, like discrete phase-sensitive demodulation, often have the small number of discrete levels - only 3 or 4 in them [1]. These levels correspond to the determined values of harmonic function with high accuracy. In figure 1 a circuit diagram of the FDAC with the FDAC with three and four discrete levels is given.

FDAC with three discrete levels (m=3) contains (Fig. 1- continuous lines) three weighting resistors of corresponding conductivities g1, g2, g3 the switching of which is performed with the help of current switches SW2, SW3 and switch SW1 of voltage +/-E from the output of the voltage source. The switches are controlled by the code coordinate signal S3=(SI; S1,3; S2,3) (Fig. 2.).

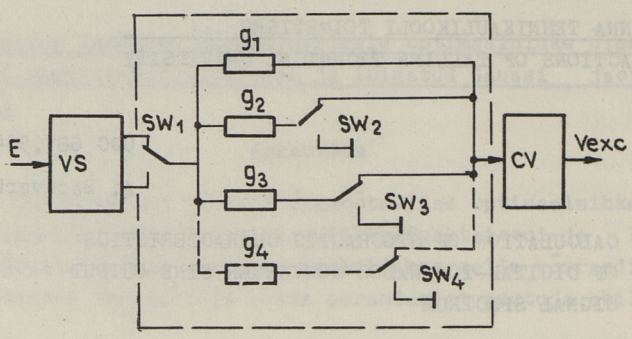

Fig. 1. Circuit diagram of the FDAC:
with three discrete levels (m=3) - continuous lines,
with four discrete levels (m=4) - continuous and dashed lines.

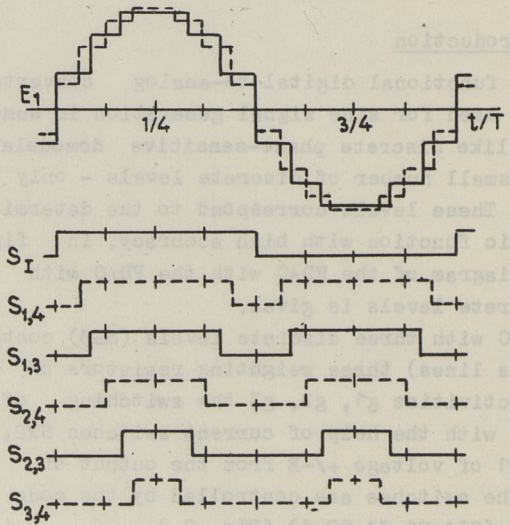

Fig. 2. Time diagrams of the variable E1 and code signals at the number of approximation levels m=3 (continuous lines) and m=4 (dashed lines).

FDAC with its four discrete levels (m=4) contains four weighting resistors (Fig. 1 - continuous and dashed lines) with corresponding conductivities of g1, g2, g3, g4. The resistors are switched on and off with the help of current switches SW1, SW2, SW3 and SW4 operating under the control of code signals S4=(SI;S1,4; S2,4; S3,4).

For determining the values of separate discrete levels the following formula is valid [2]:

$$e_q = E_o \sin [\pi/4m \cdot (2q - 1)], \qquad (1)$$

where m - the number of approximating levels,
and q - the ordinal number of the approximating level ($q=\overline{1,m}$) and the minimal value of q correspond to the lowest level of approximation.

Spectral composition of harmonic function approximated can be found according to a simple formula [2]:

$$k = 4mn \pm 1; \qquad (2)$$

and the amplitudes Ak of harmonics are the following:

$$A_k = \frac{A_1}{K},$$

where A1 is the amplitude of the first harmonic.

Spectra of the function EI at m=3 (continuous line) and at m=2 (dashed line) are shown in Fig. 3.

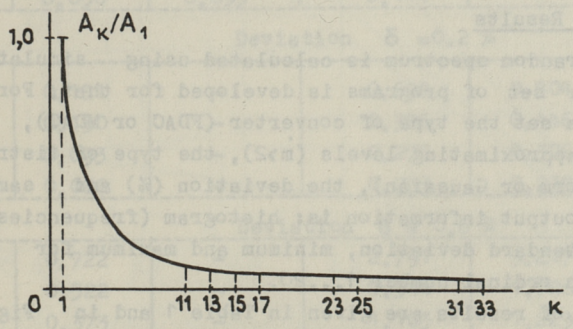

Fig. 3. Amplitude spectra of harmonic function EI approximated by three (m=3, continuous line) and four levels (m=4, dashed line).

Another possibility to generate sine signal is to use microcircuits digital-to-analog converters (MDAC) [3].

Random Deviations of the Signal Form

In a real situation it is possible to have more harmonics than according to the formula (2) (for example numbers 3, 5, 7...).

There are some causes for that:

- the discrete levels deviation from the levels which are calculated according to the formula (1);
- the step beginning time deviation from a given (calculated) time;
- the signal form deviation from a discrete step (square) form.

All these deviations in fact are random. Owing to this a signal spectrum is random too. The assignment is to calculate the random spectrum or its stochastic characteristics. At the first sight on this problem the first cause can be examined only: the discrete levels deviations from the calculated levels. Due to the necessity to eliminate the asymmetry of the output signal and to have the right level of the first harmonic, the most difficult problem is to give a right proportion for the corresponding conductivities g1... ...g4. For the microcircuits DAC, let us examine only the deviation of output signal levels and accept, that we have a possibility to give a discrete pattern in any time.

Some Results

The random spectrum is calculated using simulation methods. A set of programs is developed for that. For the calculation set the type of converter (FDAC or MDAC), the number of approximating levels ($m>2$), the type of distribution (uniform or Gaussian), the deviation (%) and sample size. The output information is: histogram (frequencies), average, standard deviation, minimum and maximum for harmonics with ordinal number 1...20.

Some of results are given in Table 1 and in Figures 4...7. All given results are for uniform distribution of

levels deviation and for sample size w=1000. The distributions of harmonics amplitudes of output signal spectrum are nearly Gaussian (Fig. 4 and Fig. 6). For MDAC the deviation 0.2 % is equal to 10-bit-MDAC with error 1 least significant bit (LSB).

Developed software make it possible to calculate statistics of harmonics of spectrum in real situation, or to calculate a needful number of levels and maximum deviation of levels for guaranty requisite level of harmonics. For example: for $Ak/A1 \leq 0.1$ % for $k=3,5,\ldots,4m-1$ needed ($p = 0.95$) FDAC with three levels of approximation and deviation ≤ 0.5 % or 10-bit-MDAC with error ≤ 0.5 LSB.

TABLE 1

Results of simulation. The standard deviation S(Ak) of amplitudes Ak of harmonics (m - number of levels, k - the ordinal number of harmonic, δ - deviation of approximating levels). S(Ak), $x10^{-3}$.

	FDAC		MDAC		
k m	3	4	3	4	8
	Deviation δ =0.1 %				
3	0.090	0.084	0.349	-	-
5	0.065	0.048	0.193	-	-
7	0.047	0.042	0.138	-	-
9	0.030	0.033	0.114	-	-
	Deviation δ =0.2 %				
3	0.181	-	0.698	0.804	1.085
5	0.130	-	0.386	0.446	0.665
7	0.093	-	0.276	0.306	0.451
9	0.060	-	0.233	0.238	0.335
	Deviation δ = 0.8 %				
3	0.722	-	2.791	3.217	4.341
5	0.522	-	1.544	1.786	2.660
7	0.373	-	1.103	1.223	1.803
9	0.242	-	0.930	0.952	1.340

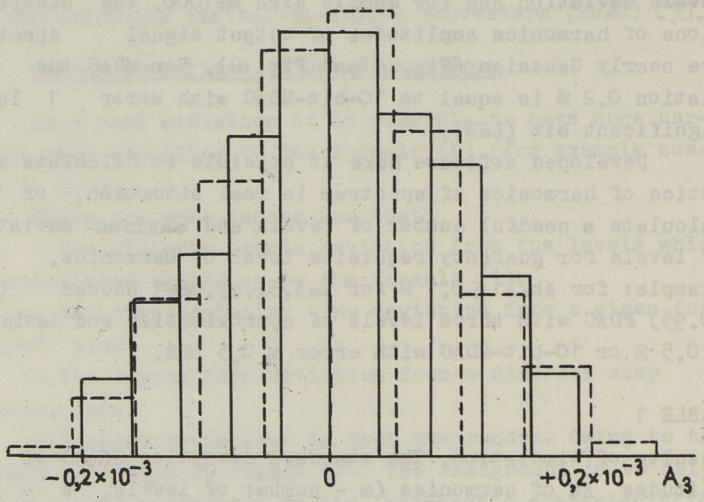

Fig. 4. Histogram for third harmonic of FDAC output sine signal. Discrete levels deviation was 0.1 %. For FDAC with three discrete levels (m=3) - continuous line and with four levels (m=4) - dashed line.

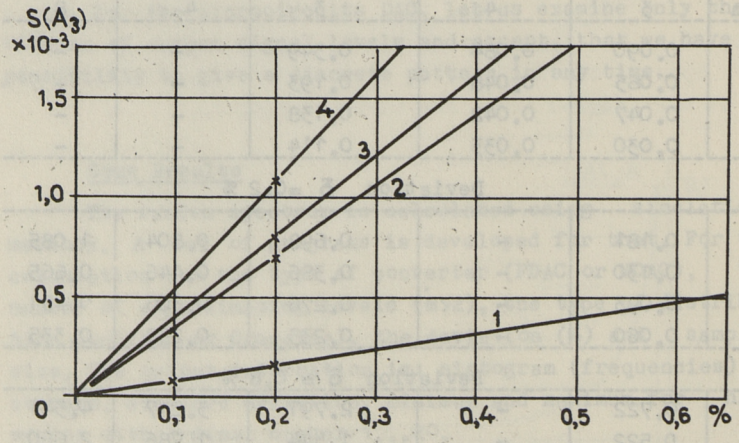

Fig. 5. Standard deviation of third harmonic amplitude S(A3) in dependence of the levels deviation.

1 - FDAC with m=3
2 - MDAC with m=3
3 - MDAC with m=4
4 - MDAC with m=8

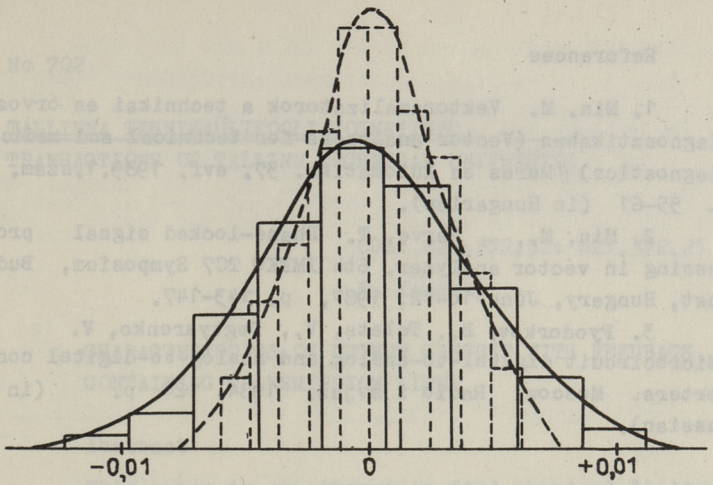

Fig. 6. Histogram for third harmonic amplitude of microcircuits DAC output sine signal. Discrete levels deviation was 0.8 %. For MDAC with three discrete levels (m=3) - dashed line, with eight levels (m=8) - continuous line.

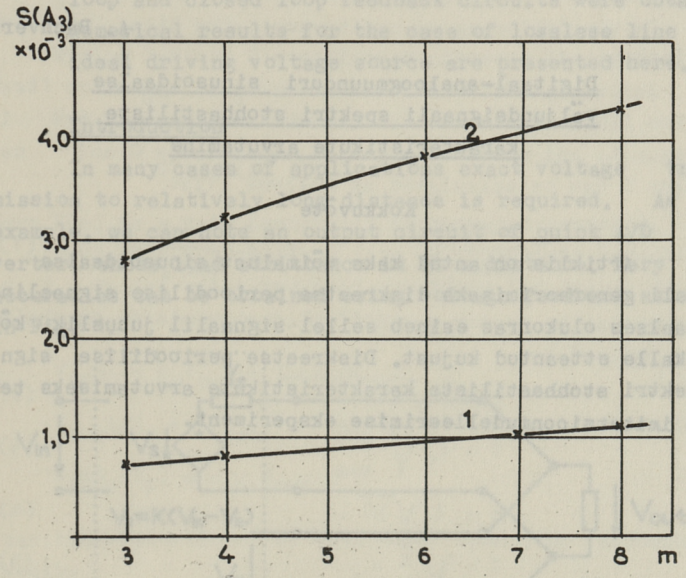

Fig. 7. Standard deviation of third harmonic amplitude of MDAC output sine signal in dependence on the number of discrete approximating levels (1 - levels deviation was 0.2 %, 2 - 0.8 %).

References

1. Min. M. Vektoranalizatorok a technikai es orvosi diagnosztikaban (Vector analyzers for technical and medical diagnostics) //Meres es Automatika. 37. evf. 1989.1.szam. P. 55-61 (in Hungarian).

2. Min, M., Parve, T. Phase-locked signal processing in vector analyzer. 6th IMEKO TC7 Symposium, Budapest, Hungary, June 10-12, 1987, p. 143-147.

3. Fyodorkov, B., Telets, V., Degtyarenko, V. Microcircuit digital-to-analog and analog-to-digital converters. Moscow: Radio i svjaz, 1984. 120 p. (in Russian).

A. Bachverk

Digitaal-analoogmuunduri sinusoidaalse väljundsignaali spektri stohhastiliste karakteristikute arvutamine

Kokkuvõte

Artiklis on antud kaks võimalust sinusoidaalse signaali genereerimiseks diskreetse perioodilise signaalina. Reaalses olukorras esineb sellel signaalil juhuslik kõrvalekalle etteantud kujust. Diskreetse perioodilise signaali spektri stohhastiliste karakteristikute arvutamiseks tehakse imitatsioonmudelleerimise eksperiment.

No 702

TALLINNA TEHNIKAÜLIKOOLI TOIMETISED
TRANSACTIONS OF TALLINN TECHNICAL UNIVERSITY

UDC: 621.372.52: 621.372.21

E. Kängsep

CHARACTERISTICS OF OUTPUT CIRCUIT WITH FEEDBACK CONTAINING TRANSMISSION LINES

Abstract

This paper is an attempt to find physical limits for feedback circuit caused by propagation time in wires from source to load. Theoretical formulae for output admittance and transfer function for both opened loop and closed loop feedback circuits were obtained. Numerical results for the case of lossless line and ideal driving voltage source are presented here.

Introduction

In many cases of applications exact voltage transmission to relatively long distance is required. As an example, we can note an output circuit of quick A/D converter, whose load admittance is at a distance. Very high accuracies can be obtained using voltage feedback as shown in Fig. 1.

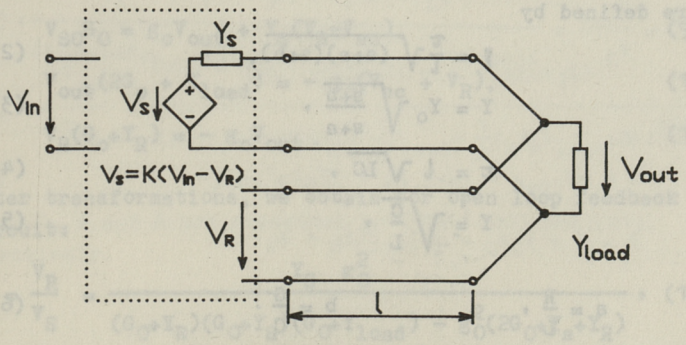

Fig. 1. Feedback circuit.

Here l is the distance of load admittance Y_{load} from the voltage source. The exact correspondence of output voltage V_{out} to input voltage V_{in} and independence from the value of load admittance Y_{load} is required. Changes of input voltage must be transferred to load admittance as precisely (accurately) as possible.

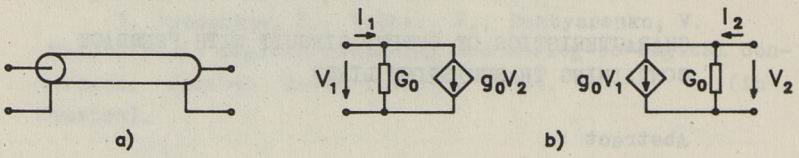

Fig. 2. Notation of transmission line (a) and its equivalent circuit (b).

Transmission Line Representation

In the following we use transmission line two-port representation, shown in Fig. 2.

Equivalent circuit admittances G_o and g_o of transmission line with series distributed resistance R and inductance L, and shunt distributed conductance G and capacitance C can be calculated as follows [1]:

$$G_o = Y \frac{\cosh \gamma l}{\sinh \gamma l}, \qquad g_o = \frac{Y}{\sinh \gamma l}. \tag{1}$$

The propagation factor γ and line characteristic admittance Y are defined by

$$\gamma = \frac{\tau}{l}\sqrt{(s+a)(s+b)}, \tag{2}$$

$$Y = Y_o \sqrt{\frac{s+b}{s+a}}, \tag{3}$$

$$\tau = l\sqrt{LC}, \tag{4}$$

$$Y = \sqrt{\frac{C}{L}}, \tag{5}$$

$$a = \frac{R}{L}, \qquad b = \frac{G}{C}. \tag{6}$$

Here τ is the delay and Y_o is the characteristic admittance on infinite frequency.

If we take into account frequency-dependence of line parameters, these equations become more complicated.

In the case of lossless line the characteristic admittance is frequency-independent and propagation factor is linear in s:

$$Y = Y_o, \quad \gamma = \frac{\tau}{t} s. \tag{7}$$

Open Loop Feedback Circuit

Hence, we proceed from general feedback circuit in Fig. 3.

The driving voltage source V_s has admittance Y_s and it is connected by the medium of transmission line T_1 with load admittance Y_{load}. Feedback voltage is transferred back from load admittance by the medium of other transmission line T_2, that is ended with receiving circuit input admittance Y_R.

During further discussions we suppose the equivalence of all parameters of both transmission lines.

For the case of closed loop feedback circuit

$$V_s = K(s)\,(V_{in} - V_R), \tag{8}$$

where K(s) is a gain (generally frequency-dependent).

Replacing transmission line by equivalent circuit in Fig. 2., we can write two-port equations for open loop general feedback circuit as follows:

$$V_{SC}G_O = g_o V_{out} + Y_S(V_S - V_{sc}), \tag{9}$$

$$V_{out}(2G_o + Y_{load}) = -\,g_o(V_{sc} + V_R), \tag{10}$$

$$V_R(G_o + Y_R) = -\,g_o V_{out}. \tag{11}$$

After transformations, we obtain for open loop feedback circuit:

$$T_S^R = \frac{V_R}{V_S} = \frac{Y_S\, g_O^2}{(G_O+Y_R)(G_O+Y_S)(G_O+Y_{load}) - g_O^2(2G_O+Y_s+Y_R)}, \tag{12}$$

$$T_S^{out} = \frac{V_{out}}{V_S} = \frac{-Y_S\, g_O(G_O+Y_R)}{(G_O+Y_R)(G_O+Y_S)(G_O+Y_{load})-g_o^2(2G_o+Y_s+Y_R)} . \quad (13)$$

Substituting G_o and g_o with (1) and after normalization by characteristic admittance

$$y_R = \frac{Y_R}{Y}, \qquad y_{load} = \frac{Y_{load}}{Y}, \quad y_S = \frac{Y_S}{Y}, \quad (14)$$

we obtain:

$$T_S^R = \frac{V_R}{V_S} = \frac{y_S \sinh \gamma l}{D}, \quad (15)$$

$$T_s^{out} = \frac{V_{out}}{V_S} = \frac{y_S(\cosh \gamma l + \sinh \gamma l)\sinh \gamma l}{D}, \quad (16)$$

where

$$D=(\cosh\gamma l+y_S\sinh\gamma l)(\cosh\gamma l+y_R\sin\gamma l)(2\cosh\gamma l+y_{load}\sinh\gamma l) -$$
$$-(2\cosh\gamma l+(y_S+y_R)\sinh\gamma l). \quad (17)$$

When $\gamma l \approx 0$, expressions (15) and (16) need division of near-zero values. The use of l'Hopital rule leads to

$$T_S^R = \frac{V_R}{V_S} = \frac{y_S}{A\cosh 2\gamma l + \frac{1}{2}y_{load} - \frac{1}{2}y_R y_S y_{load} + B\sinh 2\gamma l}, \quad (18)$$

$$T_S^{out} = \frac{V_{out}}{V_S} = \frac{y_S(\cosh \gamma l + y_R \sinh \gamma l)}{A\cosh 2\gamma l + \frac{1}{2}y_{load} - \frac{1}{2}y_R y_S y_{load} + B\sinh 2\gamma l}, \quad (19)$$

where

$$A = \frac{1}{2}y_{load} + y_R + y_S + \frac{1}{2}y_R y_S y_{load}, \quad (20)$$

$$B = 1 + y_S y_R + \frac{1}{2}y_{load}(y_R + y_S). \quad (21)$$

Transfer Function

In the case of closed loop feedback circuit with gain K(s) of controlled voltage source as in Fig. 3 and (8), we obtain:

$$T_{in}^{out} = \frac{V_{out}}{V_{in}} = \frac{K(s)\ T_S^{out}}{1 + T_S^R\ K(s)}. \qquad (22)$$

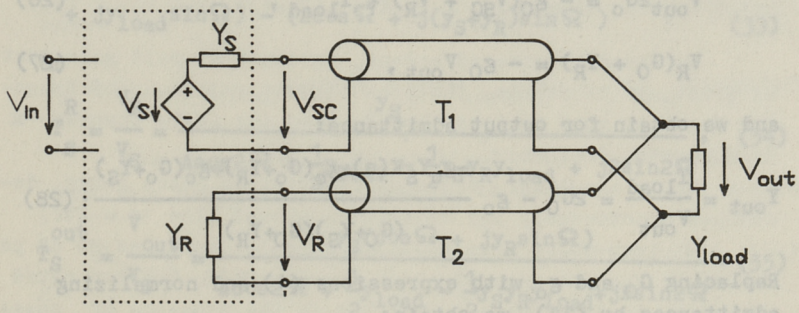

Fig. 3. General feedback circuit.

Therefore, using (15) to (21), we obtain:

$$T_{in}^{out} = \frac{V_{out}}{V_{in}} = \frac{K(s)\ y_S \sinh\gamma l\ (\cosh\gamma l + y_R \sinh\gamma l)}{K(s)\ y_S \sinh\gamma l - D} \qquad (23)$$

or

$$T_{in}^{out} = \frac{V_{out}}{V_{in}} = \frac{K(s)\ y_S\ (\cosh\gamma l + y_R \sinh\gamma l)}{K(s)y_S + A\cosh 2\gamma l + \frac{1}{2}y_{load} - \frac{1}{2}y_R y_S y_{load} + B\sinh 2\gamma l}. \qquad (24)$$

Here D, A and B are presented by (17), (20) and (21), respectively.

Output Admittance

To find output admittance, we replace load admittance Y_{load} with the current source that has current I_{load}, and taking $V_{in}=0$ in Fig. 3, and using (8) instead of (9), (10) and (11), we obtain port equations as follows:

$$- V_{SC} G_O = g_o V_{out} + Y_S(K(s)V_R + V_{SC}), \tag{25}$$

$$V_{out} 2G_o = - g_O(V_{SC} + V_R) + I_{load}, \tag{26}$$

$$V_R(G_O + Y_R) = - g_O V_{out}, \tag{27}$$

and we obtain for output admittance:

$$Y_{out} = \frac{I_{load}}{V_{out}} = 2G_O - g_o \frac{-g_o Y_S K(s) + g_o(G_o+Y_R) + g_o(G_o+Y_S)}{(G_O+Y_S)(G_O+Y_R)}. \tag{28}$$

Replacing G_O and g_o with expressions (1) and normalizing admittances by (14), we obtain:

$$Y_{out} = Y \frac{\sinh \gamma l + y_S \cosh \gamma l}{\cosh \gamma l + y_S \sinh \gamma l} + Y \frac{\sinh \gamma l + y_R \cosh \gamma l}{\cosh \gamma l + y_R \sinh \gamma l} +$$

$$+ \frac{K(s) Y_S}{(\cosh \gamma l + y_S \sinh \gamma l)(\cosh \gamma l + y_R \sinh \gamma l)}. \tag{29}$$

Feedback with Lossless Line

If lines from source to load and back are not very long, we do not commit a considerable error, supposing the lines to be lossless.

In the case of lossless transmission line, characteristic admittance is real and frequency-independent and propagation factor is imaginar and linear in frequency (7).

Therefore, substituting $s=j\omega$ and normalizing frequency by line delay

$$\Omega = \omega\tau \tag{30}$$

we obtain:

$$T_S^R = \frac{V_R}{V_S} = \frac{jy_s \sin\Omega}{d}, \qquad (31)$$

$$T_S^{out} = \frac{jy_S \sin\Omega(\cos\Omega + jy_R \sin\Omega)}{d}, \qquad (32)$$

where

$$d = (\cos\Omega + jy_S \sin\Omega)(\cos\Omega + jy_R \sin\Omega)(2\cos\Omega + jy_{load} \sin\Omega) - (2\cos\Omega + j(y_S + y_R)\sin\Omega) \qquad (33)$$

or

$$T_S^R = \frac{V_R}{V_S} = \frac{y_S}{A\cos 2\Omega + \frac{1}{2}y_{load} - \frac{1}{2}y_S y_R y_{load} + jB\sin 2\Omega}, \qquad (34)$$

$$T_S^{out} = \frac{V_{out}}{V_S} = \frac{y_S(\cos\Omega + jy_R \sin\Omega)}{A\cos 2\Omega + \frac{1}{2}y_{load} - \frac{1}{2}y_S y_R y_{load} + jB\sin 2\Omega}. \qquad (35)$$

Here A and B are given by (20) and (21).

In the same way we can obtain expressions for output admittance and transfer function of closed loop feedback circuit from (23), (24) and (29):

$$T_{in}^{out} = \frac{V_{out}}{V_{in}} = \frac{j\tilde{K}(\Omega)\, y_S \sin\Omega\, (\cos\Omega + jy_R \sin\Omega)}{j\tilde{K}(\Omega)\, y_S \sin\Omega + d}, \qquad (36)$$

$$T_{in}^{out} = \frac{V_{out}}{V_{in}} = \frac{\tilde{K}(\Omega)\, y_S \sin\Omega\,(\cos\Omega + jy_R \sin\Omega)}{y_S\tilde{K}(\Omega) + A\cos 2\Omega + \frac{1}{2}y_{load} - \frac{1}{2}y_S y_R y_{load} + jB\sin 2\Omega}, \qquad (37)$$

$$Y_{out} = Y\frac{j\sin\Omega + y_S\cos\Omega}{\cos\Omega + jy_S\sin\Omega} + y\frac{j\sin\Omega + y_R\cos\Omega}{\cos\Omega + jy_R\sin\Omega} + \frac{\tilde{K}(\Omega)\; Y_S}{(\cos\Omega + jy_S\sin\Omega)(\cos\Omega + jy_R\sin\Omega)}. \qquad (38)$$

Here $\tilde{K}(\Omega)$ is the gain of controlled voltage source in Fig. 3 and (8).

Stability of Feedback Circuit

According to Nyquist's criterion of stability [2], closed loop feedback circuit is stable, when curve of open loop feedback circuit transfer function intersects real axis to the left of the point 1:

$$|K(s)||T_S^R|<1, \text{ when } \arg T_S^R + \arg K(s)=(2k+1)\pi, \quad k=0,1,\ldots \quad (39)$$

In order to give advantage, feedback circuit gain must be great. To be stable, the open circuit magnitude of transfer function must be less than 1, when its phase changes $-\pi$ from zero'th frequency.

As we see later, transfer function T_S^R phase curve decreases monotonously and oscillates around line $\varphi=-2\Omega$.

Minimum-phase gain $K(j\omega)$ magnitude decreases 20 dB per decade in the presence of phase change $-\pi/2$. Greater rates of magnitude decrease are possible in the presence of phase change $-\pi$ and more.

Therefore, to guarantee feedback circuit stability, we can use only first order integrator for realizing K(s). This causes phase change $-\pi/2$ and other $-\pi/2$ remain for delay in the transmission line (for T_S^R).

Hence, to determine the bounds of stability, we are interested in further discussions to find frequency, when phase change on line ($\arg T_S^R$) is $-\pi/2$ and magnitude of transfer function T_S^R on this frequency.

Expression for general feedback circuit (34) is too complicated to understand all its properties. So we observe simpler special cases of feedback circuit.

Special Cases

In the following we suppose lossless line and all admittances in Fig. 3 to be real.

When driving voltage source admittance is much greater than line characteristic admittance (when we can suppose the source to be practically ideal), then it can be neglected without causing remarkable errors:

$$T_S^R = \lim_{y_S \to \infty} \frac{V_R}{V_S} = \frac{1}{d_S} . \qquad (40)$$

$$T_S^{out} = \lim_{y_S \to \infty} \frac{V_{out}}{V_S} = \frac{\cos\Omega + jy_R \sin\Omega}{d_S} . \qquad (41)$$

$$T_{in}^{out} = \lim_{y_S \to \infty} \frac{V_{out}}{V_{in}} = \frac{\tilde{K}(\Omega)\,(\cos\Omega + jy_R \sin\Omega)}{\tilde{K}(\Omega) + d_S} , \qquad (42)$$

where

$$d_S = (1 + \frac{1}{2}y_R y_{load})\cos 2\Omega - \frac{1}{2}y_R y_{load} + j(y_R + \frac{1}{2}y_{load})\sin 2\Omega . \qquad (43)$$

Now we determine the critical point for stability: when $\varphi = \arg T_S^R = -\pi/2$, then d_S is imaginar and we obtain:

$$\Omega\Big|_{\varphi = \frac{\pi}{2}} = \frac{1}{2} \arccos \frac{\frac{1}{2}y_R y_{load}}{1 + \frac{1}{2}y_R y_{load}} , \qquad (44)$$

and the magnitude of transfer function is:

$$\left|T_S^R\right|\Big|_{\varphi = -\frac{\pi}{2}} = \frac{1 + \frac{1}{2}y_R y_{load}}{(y_R + \frac{1}{2}y_{load})\sqrt{1 + \frac{1}{2}y_R y_{load}}} . \qquad (45)$$

By expressions (44) and (45) we can determine frequency, when the phase of transfer function is $-\pi/2$ and its magnitude at this frequency.

During further discussions we suppose the driving voltage source to be ideal ($y_S = \infty$).

Case 1: $y_{load} = 0$.

In this case feedback circuit is without load, and we get from (40) the following expression:

$$T_S^R\Big|_{\substack{y_{load}=0 \\ y_S=\infty}} = \frac{V_R}{V_S} = \frac{1}{\cos 2\Omega + jy_R \sin 2\Omega} . \qquad (46)$$

Frequency responses for some values of normed receiver admittance y_R are given in Fig. 4.

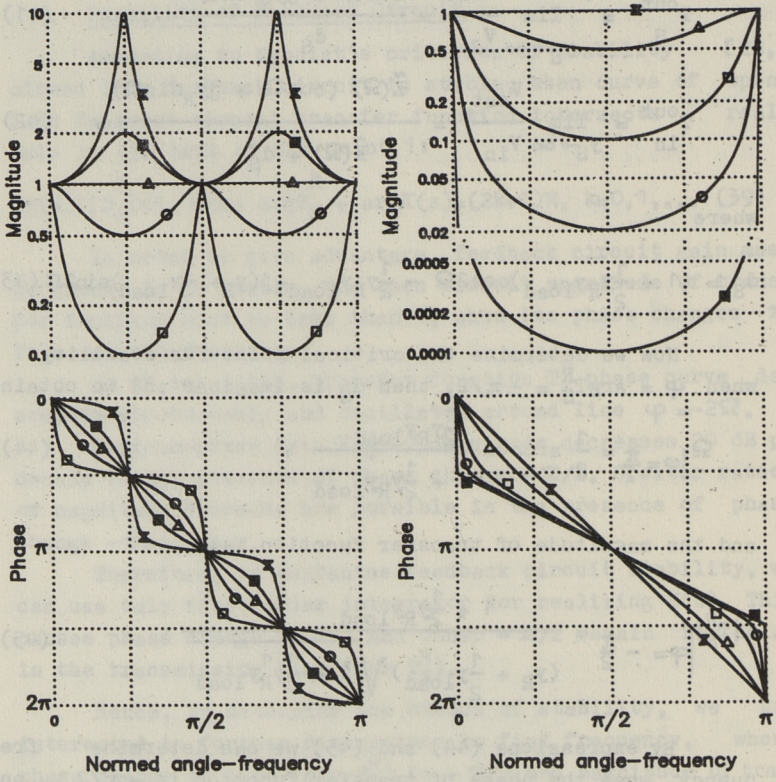

Fig. 4. Open loop without load feedback circuit transfer function from driving source to receiver.

△ – y_R=1 ,
□ – y_R=10 ,
○ – y_R=2 ,
■ – y_R=0.5 ,
⧗ – y_R=0.1 .

Fig. 5. On receiver side matched open loop feedback circuit transfer function from driving source to receiver.

△ – y_{load} = 1 ,
□ – y_{load} = 9 ,
○ – y_{load} = 49 ,
■ – y_{load} = 9999 ,
⧗ – y_{load} = 0 .

As we can see, matched line (y_R=1) has frequency-independent magnitude of transfer function and its phase is linear (delay is frequency-independent).

In the case of unmatched line magnitude of transfer function has extremes at

$$\Omega = k\frac{\pi}{4}, \qquad k=0,1,... \tag{47}$$

Case A: $y_R > 1$, magnitude of transfer function has minimum

$$\left|T_S^R\right|_{min} = \frac{1}{y_R}, \qquad \Omega = (2k+1)\frac{\pi}{4}, \quad k=0,1,... \tag{48}$$

and maximum

$$\left|T_S^R\right|_{max} = 1, \qquad \Omega = k\frac{\pi}{2}, \qquad k=0,1,... \tag{49}$$

Case B: $y_R < 1$, magnitude of transfer function has minimum

$$\left|T_S^R\right|_{min} = 1, \qquad \Omega = k\frac{\pi}{2}, \qquad k=0,1,... \tag{50}$$

and maximum

$$\left|T_S^R\right|_{max} = \frac{1}{y_R}, \qquad \Omega = (2k+1)\frac{\pi}{4}, \quad k=0,1,... \tag{51}$$

In both cases the phase curve oscillates around matched line phase curve and intersects it at points

$$\Omega = k\frac{\pi}{4}, \qquad k=0,1,... \tag{52}$$

At normed angle-frequency $\Omega = \pi/4$ phase and magnitude of transfer function are $\varphi = \pi/2$ and

$$\left|T_S^R\right|_{\varphi = -\frac{\pi}{2}} = \frac{1}{y_R} \tag{53}$$

respectively.

It means that to guarantee stability,

1) the receiver must have non-zero admittance ($Y_R \neq 0$);
2) the time constant of gain must be greater, when receiver admittance is less.

Case 2: $y_R = 0$.

In this case feedback circuit receiver admittance is zero (receiver impedance is much greater than line characteristic impedance) and from (40) we obtain:

$$T_S^R \Big|_{\substack{y_R=0 \\ y_S=\infty}} = \frac{V_R}{V_S} = \frac{1}{\cos 2\Omega + j\frac{1}{2}y_{load}\sin 2\Omega} \cdot \quad (54)$$

Comparing (54) with (46), we establish that if we put y_{load} instead of y_R, then this case become equivalent to the previous case.

Case 3: $y_R = 1$.

In this case the line is matched from receiver side ($y_R=1$) and from (40) we obtain:

$$T_S^R \Big|_{\substack{y_R=1 \\ y_S=\infty}} = \frac{V_R}{V_S} = \frac{1}{(1+\frac{1}{2}y_{load})\cos 2\Omega - \frac{1}{2}y_{load} + j(1+\frac{1}{2}y_{load})\sin 2\Omega} \cdot \quad (55)$$

Frequency responses for some values of load admittance are given in Fig. 5.

If $Y_{load} > 0$, then magnitude of transfer function T_S^R has maximum

$$\left| T_S^R \right|_{max} = \left| \frac{V_R}{V_S} \right| = 1, \quad \Omega = k\pi, \quad k=0,1,\ldots \quad (56)$$

and minimum

$$\left| T_S^R \right|_{min} = \left| \frac{V_R}{V_S} \right| = \frac{1}{(1+y_{load})}, \quad \Omega = (2k+1)\frac{\pi}{2}, \quad k = 0,1,\ldots \quad (57)$$

Phase curve oscillates around without-load-circuit phase curve and intersects it at points

$$\Omega = k\frac{\pi}{2}, \quad k=0,1,\ldots \quad (58)$$

Transfer function T_S^R phase $\varphi = -\pi/2$ at frequency

$$\Omega\Big|_{\varphi=-\frac{\pi}{2}} = \frac{1}{2}\arccos\frac{\frac{1}{2}y_{load}}{1+\frac{1}{2}y_{load}} \qquad (59)$$

and magnitude of transfer function T_S^R at this frequency is

$$\left|T_S^R\right|\Big|_{\varphi=-\frac{\pi}{2}} = \left|\frac{V_R}{V_S}\right| = \frac{1}{\sqrt{1+y_{load}}}. \qquad (60)$$

Case A: $y_S >> 1$.

From (59) and (60) we obtain

$$\Omega\Big|_{\substack{\varphi=-\frac{\pi}{2}\\ y_S>>1}} \approx \frac{1}{\sqrt{y_{load}}}, \qquad (61)$$

$$\left|T_S^R\right|\Big|_{\substack{\varphi=-\frac{\pi}{2}\\ y_S>>1}} \approx \frac{1}{\sqrt{y_{load}}}. \qquad (62)$$

If we suppose the gain (8) to be ideal integration function,

$$\tilde{K}(\Omega) = \frac{Const}{j\Omega}, \qquad (63)$$

then we obtain for magnitude of open loop feedback circuit at a critical frequency of stability (phase is π)

$$\left|T_S^R\right|\left|\tilde{K}(\Omega)\right|\Big|_{\substack{y_S>>1\\ \Omega=1/y_{load}}} \approx Const \qquad (64)$$

It means that to guarantee feedback circuit stability, the line delay normed time constant of the gain must always be greater than direct voltage gain.

In Fig.6, the Nyquist diagram is given for open loop feedback circuit transfer function for gain

$$\tilde{K}(\Omega) = \frac{1000}{1 + j4600\Omega} \quad . \tag{65}$$

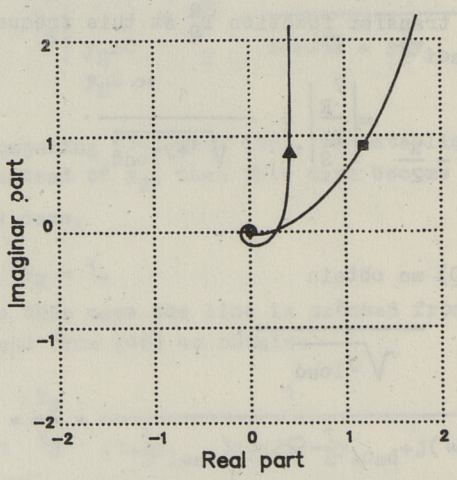

Fig. 6. Nyquist diagram of open loop feedback circuit, matched on receiver side.

▲ – without load,
■ – $y_{load}=10$.

As we see in Fig. 6, in case of loaded feedback circuit, the curve of open loop transfer function ($T_S^R \tilde{K}(\Omega)$) passes by point 1 in real axis nearer than in loadless case.

From this we can draw the conclusion that the load can decrease stability of feedback circuit or make the circuit unstable.

Case 4: $y_R \neq 1$, $y_{load} \neq 0$.

In this case, the expression (40) is valid. Transfer function T_S^R ourves for two values of y_R are shown in Fig. 7 ($y_R=5$) and in Fig. 8 ($y_R=0.2$).

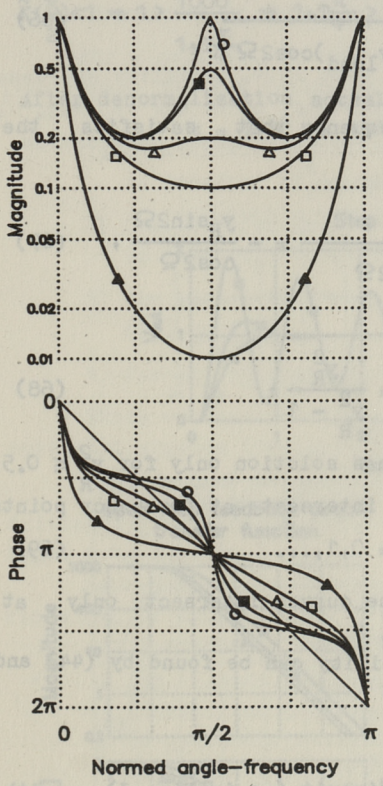

Fig. 7. Open loop feedback circuit transfer function from driving source to receiver. $y_R = 5$.

○ – $y_{load} = 0$,
■ – $y_{load} = 0.2$,
□ – $y_{load} = 9/5$,
△ – $y_{load} = 0.9$,
▲ – $y_{load} = 99/5$.

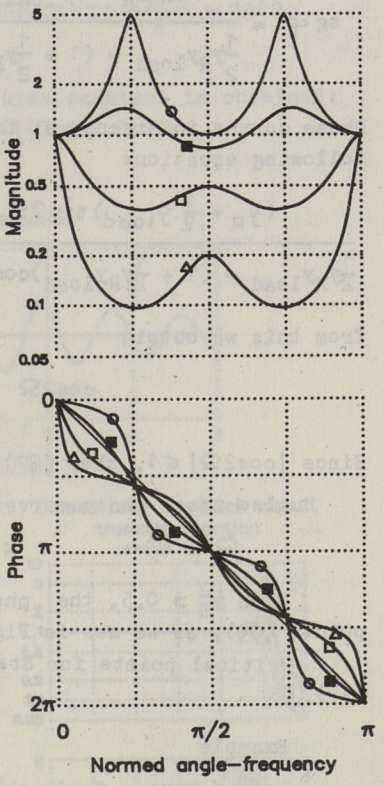

Fig. 8. Open loop feedback circuit transfer function from driving source to receiver. $y_R = 0.2$.

○ – $y_{load} = 0$,
■ – $y_{load} = 1$,
□ – $y_{load} = 5$,
△ – $y_{load} = 20$.

As we can see, the phase curve of transfer function T_S^R oscillates around without load circuit curve. To find points of intersection, we derive from (40) the tangent of phase of transfer function ($\varphi = \arg T_S^R$):

$$\operatorname{tg}\varphi = \frac{(y_R + \frac{1}{2}y_{load})\sin 2\Omega}{\frac{1}{2}y_R y_{load} - (1 + \frac{1}{2}y_R y_{load})\cos 2\Omega}. \qquad (66)$$

Phase curves intersect at frequency that satisfies the following equation:

$$\frac{(y_R + \frac{1}{2}y_{load})\sin 2\Omega}{\frac{1}{2}y_R y_{load} - (1 + \frac{1}{2}y_R y_{load})\cos 2\Omega} = -\frac{y_R \sin 2\Omega}{\cos 2\Omega}, \qquad (67)$$

from this we obtain

$$\cos 2\Omega = \frac{y_R^2}{y_R^2 - 1}. \qquad (68)$$

Since $|\cos 2\Omega| \leq 1$, then (67) has solution only for $y_R^2 \leq 0.5$.

Also these phase curves intersect at frequency points

$$\Omega = k\frac{\pi}{2}, \qquad k = 0,1,... \qquad (69)$$

When $y_R^2 > 0.5$, the phase curves intersect only at points (69), as we see in Fig. 7.

Critical points for stability can be found by (44) and (45).

Example

Let us have a feedback circuit (as in Fig. 3) with lossless transmission line, where: $Y_S \to \infty$, $Y=150\Omega$, $\tau = 100ns$ ($l=20m$), $Y_R=150\Omega$, $Y_{load}=0$.

From (44) we obtain

$$\Omega\Big|_{\varphi = -\frac{\pi}{2}} = \frac{1}{2}\arccos\frac{0}{1+0} = \frac{\pi}{4},$$

$$\left|T_S^R\right|_{\varphi = -\frac{\pi}{2}} = 1.$$

Let

$$\tilde{K}(S) = \frac{C}{1 + T\Omega},$$

if we put c=1000, then by (39) we obtain

$$\tilde{K}(\frac{\pi}{2})<1 \Rightarrow 1 > \frac{1000}{1+T\frac{\pi}{4}} \Rightarrow 1+T\frac{\pi}{4} > 1000 \Rightarrow T > \frac{999 \cdot 4}{\pi} \approx 1300.$$

After denormalization actual time constant is obtained:

$$t = T \cdot \tau = 1300 \cdot 100ns = 0.13ms.$$

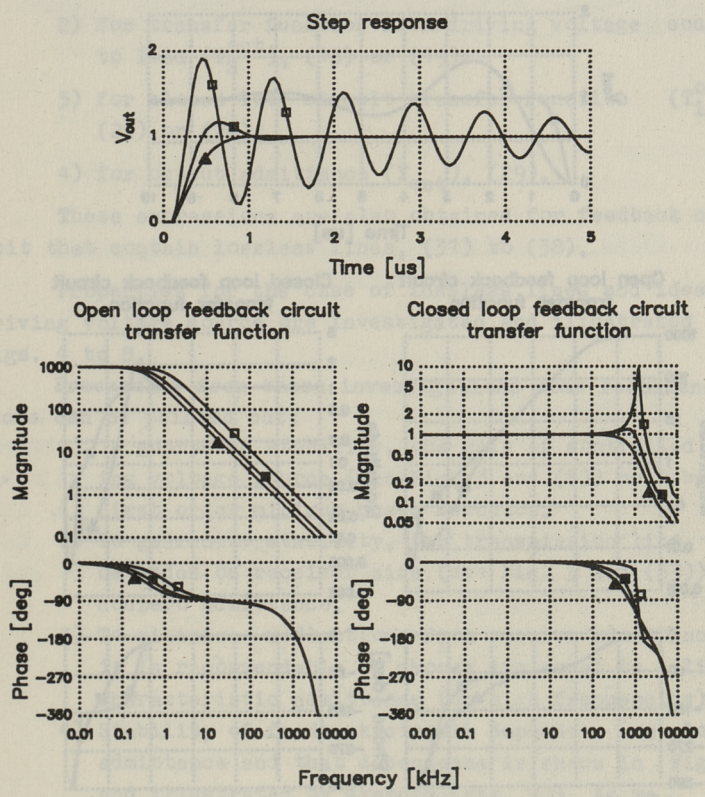

Fig. 9. Without load feedback circuit with transmission line, matched on receiver side. Line delay is 100ns (length is 20 meters) and characteristic impedance is 150 Ohms. Gain is 1000.

▲ – gain time constant is 0.46ms,
■ – gain time constant is 0.3ms,
□ – gain time constant is 0.14ms.

To guarantee stability, we put t=0.14ms and obtain characteristics, shown in Fig. 9.

As we see, the step response is oscillating. To avoid oscillation, time constant of gain must be increased to t= =0.46ms.

If the circuit is loaded with 15 Ω, stability decreases and step response becomes oscillating, as we see in Fig. 10. That phenomenon corresponds to the above given discussions and with Fig. 6.

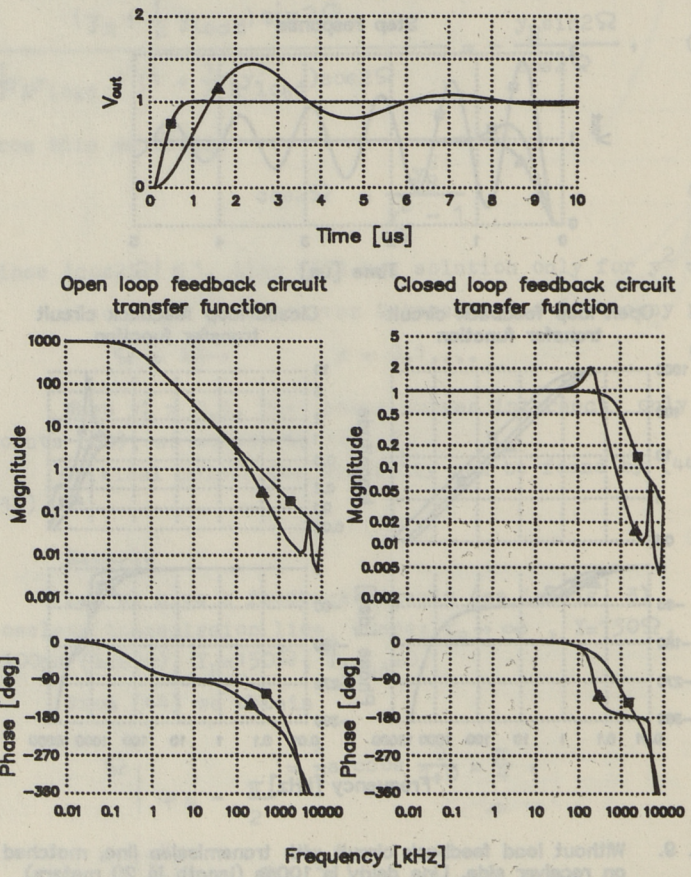

Fig. 10. Feedback circuit with transmission line, matched on receiver side. Line delay is 100ns (length is 20 meters) and characteristic impedance is 150 Ohms. Gain is 1000 and gain time constant is 0.46ms.
▲ – without load,
■ – with load 15 Ohms.

Conclusion

For a general feedback circuit containing transmission lines (Fig. 3), the following expressions are obtained:

1) for transfer function from driving voltage source to receiver (T_S^R), (12) or (18);

2) for transfer function from driving voltage source to load (T_S^{out}), (13) or (19);

3) for closed loop circuit transfer function (T_{in}^{out}), (23) or (24);

4) for output admittance (Y_{out}), (29).

These expressions are also obtained for feedback circuit that contain lossless lines, (31) to (38).

Properties for the case of lossless lines and ideal driving voltage source are investigated and illustrated by Figs. 4 to 8.

Proceeding from these investigations some recommendations can be pointed out:

1) To guarantee stability, the gain of controlled driving voltage source (see Fig. 3 and (8)) must be a first order minimum-phase function.

2) To guarantee stability, the transmission line must be ended on receiver side (see Fig. 3 and (53)) with nonzero admittance.

3) To minimize reflections from receive admittance, it is recommendable to choose its equal to line characteristic admittance (on high frequencies).

4) Stability of feedback circuit depends on load admittance and that dependence is shown in Fig. 6 and illustrated by example (Fig. 10). As we see, load admittance exists, for which the stability has minimum. To guarantee stability for all available loads, we must choose sufficiently great time constant for gain of controlled driving voltage source.

This paper does not contain discussions about the influence of value of driving voltage source admittance to

properties of feedback circuit. This is a good matter for further investigations.

References

1. Mayer, D. Uvod do teorie elektrickych obvodu. Praha: SNTL-ALFA, 1981.

2. Cajka, J. Kvasil, J. Teorie linearnich obvodu. Praha: SNTL-ALFA, 1979.

E. Kängsep

Pikki liine sisaldava tagasisidega väljundahela karakteristikud

Kokkuvõte

Käesolev artikkel on katse leida tagasisidega ahela omaduste füüsikalisi piire, mis on tingitud laine levimise ajast allikast koormusele. Artiklis on tuletatud väljundjuhtivuse ja ülekandefunktsiooni teoreetilised valemid nii avatud kui ka suletud tagasisideahelaga sidu jaoks. Kadudeta liini ja ideaalse pingeallika erijuhu jaoks on esitatud numbrilised tulemused.

No 702

TALLINNA TEHNIKAÜLIKOOLI TOIMETISED
TRANSACTIONS OF TALLINN TECHNICAL UNIVERSITY

UDC: 621.372.5

E. Kängsep

GENERAL CHARACTERISTIC MODEL OF LINEAR TIME-INVARIANT TWO-PORTS

Abstract

This paper is an attempt to find a general characteristic model of linear time-invariant two-ports, for applications in time domain analysis. The convolution model of transmission line presented by M. Valtonen and used by other authors is the special application of the model presented here.

General Characteristic Model

Let us start from a two-port, shown in Fig. 1 and described by the characteristic parameters [3]:

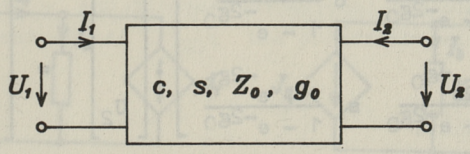

Fig. 1. Two-port.

$$\frac{1}{Z_0 \sinh g_0}\begin{bmatrix} \cosh g_0 & -c \\ -\frac{1}{c} & s\cosh g_0 \end{bmatrix}\cdot\begin{bmatrix} U_1 \\ U_2 \end{bmatrix}=\begin{bmatrix} I_1 \\ I_2 \end{bmatrix}, \quad (1)$$

the two-port characteristic impedance Z_0 is defined by

$$Z_0 = \sqrt{Z_{01}Z_{02}}\,. \qquad (2)$$

Here Z_{01} and Z_{02} are the characteristic impedances from the first and second port, respectively.

The propagation factor g_0 is presented by

$$g_0 = \frac{1}{2}\ln\frac{U_1I_1}{U_2I_2}, \qquad (3)$$

the coefficient of asymmetry s of the two-port is defined as

$$s = \sqrt{\frac{Z_{01}}{Z_{02}}} \qquad (4)$$

and the coefficient of reciprocity c is defined as

$$c = \sqrt{|A|}\,. \qquad (5)$$

Here A is the scattering matrix of the two-port.

Rewriting the hyperbolic functions to have exponents only, we obtain:

$$\frac{1}{Z_0}\begin{bmatrix} \frac{1}{s}\,\frac{1+e^{-2g_0}}{1-e^{-2g_0}} & c\,\frac{-2e^{-g_0}}{1-e^{-2g_0}} \\ \frac{1}{c}\,\frac{-2e^{-g_0}}{1-e^{-2g_0}} & s\,\frac{1+e^{-2g_0}}{1-e^{-2g_0}} \end{bmatrix} \cdot \begin{bmatrix} U_1 \\ U_2 \end{bmatrix} = \begin{bmatrix} I_1 \\ I_2 \end{bmatrix} \qquad (6)$$

or

$$\frac{1}{Z_0(1-e^{-g_0})}\begin{bmatrix} 1 & \frac{1}{s}e^{-g_0} \\ -\frac{s}{c}e^{-g_0} & -\frac{1}{c} \end{bmatrix} \cdot \begin{bmatrix} \frac{1}{s} & -c\,e^{-g_0} \\ e^{-g_0} & -sc \end{bmatrix} \cdot \begin{bmatrix} U_1 \\ U_2 \end{bmatrix} = \begin{bmatrix} I_1 \\ I_2 \end{bmatrix} \qquad (7)$$

After multiplicating both sides of the equation by inverse matrix on the left hand we obtain:

$$\frac{1}{Z_0}\begin{bmatrix} \frac{1}{s} & -c\,e^{-g_0} \\ e^{-g_0} & -sc \end{bmatrix}\cdot\begin{bmatrix} U_1 \\ U_2 \end{bmatrix} = \begin{bmatrix} 1 & \frac{c}{s}e^{-g_0} \\ -se^{-g_0} & -c \end{bmatrix}\cdot\begin{bmatrix} I_1 \\ I_2 \end{bmatrix} \quad (8)$$

Using characteristic admittances instead of characteristic impedances

$$Y_0 = \frac{1}{Z_0}, \qquad Y_{01} = \frac{1}{Z_{01}}, \qquad Y_{02} = \frac{1}{Z_{02}} \quad (9)$$

we obtain:

$$Y_0\left(\frac{1}{s}U_1 - c\,e^{-g_0}U_2\right) = I_1 + \frac{c}{s}e^{-g_0}I_2, \quad (10a)$$

$$Y_0\left(e^{-g_0}U_1 - s\,c\,U_2\right) = -s\,e^{-g_0}I_1 - c\,I_2. \quad (10b)$$

With the use of (2), (4) and (9):

$$I_1 = Y_{01}U_1 - \frac{c}{s}e^{-g_0}\left[Y_{02}U_2 + I_2\right], \quad (11a)$$

$$I_2 = Y_{02}U_2 - \frac{s}{c}e^{-g_0}\left[Y_{01}U_1 + I_1\right]. \quad (11b)$$

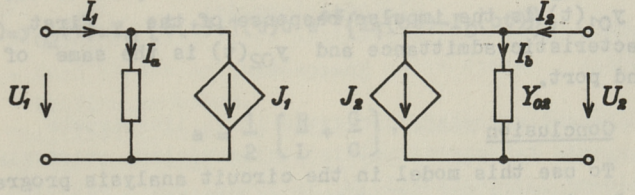

Fig. 2. Characteristic model of two-port.

These equations lead us to the model in Fig. 2, where

$$J_1 = -\frac{c}{s}e^{-g_0}\left[2I_b + J_2\right], \quad (12a)$$

$$J_2 = -\frac{s}{c}e^{-g_0}\left[2I_a + J_1\right]. \quad (12b)$$

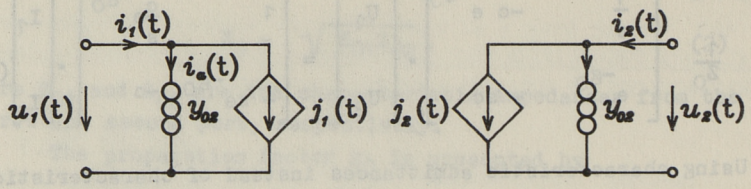

Fig. 3. Characteristic model of two-port in time domain.

In time domain the model in Fig. 3 is obtained, which is described by equations as follows:

$$j_1(t) = i_{21}(t) * \left[2i_b(t) + j_2(t) \right], \qquad (13a)$$

$$j_2(t) = i_{12}(t) * \left[2i_a(t) + j_1(t) \right], \qquad (13b)$$

$$i_a(t) = y_{01}(t) * u_1(t), \qquad (14a)$$

$$i_b(t) = y_{02}(t) * u_2(t). \qquad (14a)$$

Here "*" denotes the convolution, $i_{21}(t)$ is the impulse response of matched two-port from the second port to the first one and $i_{12}(t)$ is the same from the first port to the second one. $y_{01}(t)$ is the impulse response of the first port characteristic admittance and $y_{02}(t)$ is the same of the second port.

Conclusion

To use this model in the circuit analysis program for time domain analysis of mixed lumped and distributed circuits the two-port must be replaced by an equivalent circuit, shown in Fig. 4.

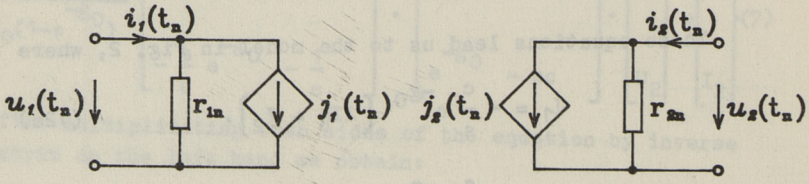

Fig. 4. Two-port equivalent circuit at the n-th time step.

Currents of sources and conductances of resistors can be calculated by the use of numerical calculation of convolutions in each time step t_n.

The advantage of this model is that all required impulse responses are for a matched two-port, without reflections on ports. For this reason the impulse responses attenuate more quickly and numerical calculation of convolutions requires a less number of integration steps than with other model structures.

Here we do not discuss numerical methods for calculation of convolution and methods for finding required impulse responses. These problems are a good matter for other papers and investigations.

Appendix

The Transmission Line Model

In the case of transmission line the impulse responses for characteristic model are given by [1], [2], [4]:

$$i_{21}(t) = i_{12}(t) = e^{-at}\,\delta(t-\tau)+1(t-\tau)\frac{b\tau e^{-at}}{\sqrt{t^2-\tau^2}}\,I_1(b\sqrt{t^2-\tau^2}), \quad (15)$$

$$y_{01}(t)=y_{02}(t)=Y_0\left\{\delta(t)+1(t)b\,e^{at}\{I_1(bt)-I_0(bt)\}\right\}, \quad (16)$$

where

$$a = \frac{1}{2}\left[\frac{R}{L}+\frac{G}{C}\right], \quad (17)$$

$$b = \frac{1}{2}\left[\frac{R}{L}-\frac{G}{C}\right], \quad (18)$$

$$\tau = l\sqrt{LC}, \quad (19)$$

$$Y_0 = \sqrt{\frac{C}{L}}. \quad (20)$$

Here $\delta(t)$ is the Dirack's impulse function, $1(t)$ is the Heaviside eigen step function, $I_0(t)$ and $I_1(t)$ are the first kind modified Bessel's functions of zero'th and first order, respectively. Transmission line series distributed resistance and inductance are R and L, respectively, and

shunt distributed conductance and capacitance are G and C, respectively. τ is the delay and Y_0 is the characteristic admittance on infinite frequency.

References

1. Valtonen M. Computer-aided analysis of mixed lumped and distributed circuits in time domain. // Proc. of IEEE CAS Conf. New York, 1978.

2. Uhle M. Transientanalyse nichtlinear dynamischer Netzwerke mit verlustbehaften elektrischen Leitungen // Nachrichtentechnik Elektronik. 1983. B. 33, Nr. 12.

3. Mayer D. Úvod do teorie elektrických obvodů. Praha: SNTL-ALFA, 1981.

4. Kängsep, E. Simulace soustav se rosprostřenými parametry. Diplomová práce. Praha: ČVUT, 1985.

E. Kängsep

Lineaarsete ajas muutumatute kaksportide üldine lainemudel

Kokkuvõte

Käesolev artikkel on katse leida lineaarsete ajas muutumatute kaksportide üldist lainemudelit, eesmärgiga kasutamiseks aja-analüüsil. M. Valtoneni poolt esitatud ja ka teiste autorite poolt kasutatud pika liini konvolutsioonimudel on siin esitatud mudeli erijuht.

No 702

TALLINNA TEHNIKAÜLIKOOLI TOIMETISED
TRANSACTIONS OF TALLINN TECHNICAL UNIVERSITY

UDC 621.317.727.1

R. Joers, J. Peterson

VOLTAGE RATIO ERROR ESTIMATION IN RATIO TRANSFORMERS

Abstract

The error estimation in inductively coupled voltage dividers are examined and equations are developed from which the voltage ratio error may be predicted.

Ratio transformers possess a high accuracy of A.C. voltage and current ratio which are determined by the turns ratio and caused by a special performance of the transformer's windings. The ratio transformer used in A.C. voltage calibrators are slightly loaded and they are applied as inductive voltage dividers (IVD).

Problems, which arise in IVD designing and application, include:

- voltage ratio error estimation in a single stage;
- load effect estimation and multi stage interconnection problems.

The first problem is concerned about the IVD inequalities of the sectional windings. IVD instrument error at low frequences is determined by scattering the parameters in the sections and the ferromagnetic core's characteristics. An analysis of IVD transmission errors in the low frequency field of sinusoidal signals, originating from the transformer's model, containing its own and mutual impedances of the sections windings has been discussed by Baikov and Bazilevich [1, 2].

However, we are often interested in a few special problems, e.g.: the calculation of transmission error components, caused by the scattering of active resistances of the windings. This kind of calculation is made more difficult because of complicated dependances on the capacity of losses and

the core's permeability from the signal's frequency and amplitude.

Let us look at one of the IVD stages, whose all n sections are carried out by windings and switched on in sequence. Then we can show that this transmission coefficient of the IVD voltage, which from the input embraces all n sections towards output, embracing m sections, is accurately determined by the ratio:

$$K_{um} = \frac{m}{n} + \left(\sum_{1}^{m} z_i - \frac{m}{n} \sum_{1}^{n} z_i \right) \cdot Y_{iN}, \qquad (1)$$

where the first component characterizes the geometrical coefficient of the transmission (the ratio of windings), and the second one determines transmission error, caused by the effect of scattering impedances in section Z_i and the input conductivity of IVD Y_{IN}. Impedance of i section Z_i contains active resistance r_i and leakage inductance L_i in the given section.

The equation (1) allows us to estimate the error, when IVD transmissions of A.C. differ from the ones of D.C., and it would be sensible to use it in the following cases:

1. On the basis of non-complicated measurements of input conductivity $Y_{IN}(\omega)$ and for determining the summary deviation of active resistance Δr_m for the section from 1 to m, from the mean resistance, we can then determine the transmission coefficient as:

$$K_{um}(\omega) = \frac{m}{n} + \Delta r_m \cdot Y_{IN}(\omega)$$

and from here it will be easy to pass on to the ratio and phase angle error calculation. The results of the corresponding transmission calculations for the experimental IVD are presented in Fig. 1, curve a. As can been seen, frequency dependence of error is not subjected to the law f^{-2} and, on the whole, is determined by the losses in the core.

2. The designs of IVD stages are known, where some

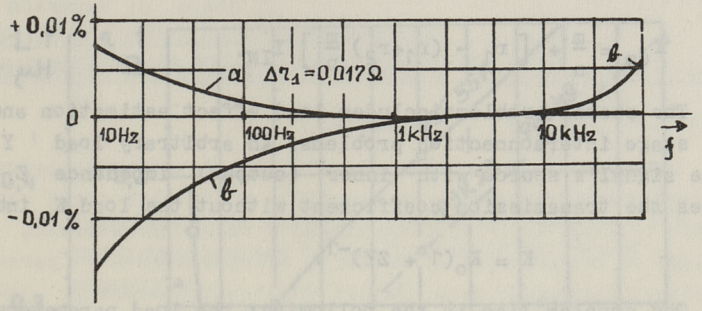

Fig. 1.

sections are carried out with shunt (parallel) similar windings. The corresponding transmissions for the diagram in Fig. 2,a are depicted then according to (1), by the formulae:

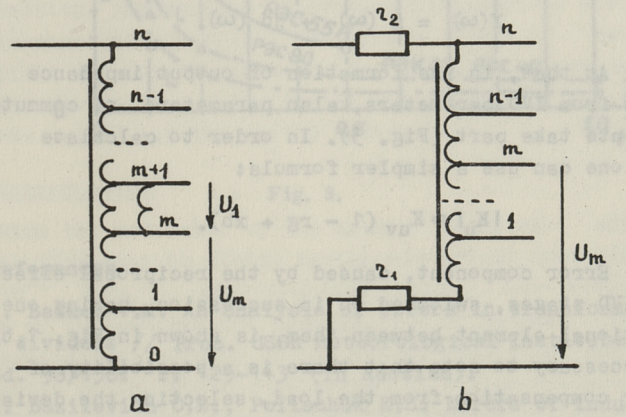

Fig. 2.

$$K_{u1} = \frac{1}{n} - \frac{n-1}{2n} z \cdot Y_{IN},$$

$$K_{um} = \frac{m}{n} + \frac{1}{2} \cdot \frac{m}{n} \cdot z \cdot Y_{IN}.$$

3. Resistance effect estimation of coupling circuits r_1, r_2 (Fig. 2 b) is described by the formula:

$$K_{um} = \frac{m}{n} + \left[r_1 - (r_1 + r_2) \frac{m}{n} \right] Y_{IN}.$$

The second problem includes load effect estimation and multi stage interconnection problems. An arbitrary load Y on the signal's source with inner (output) impedance Z changes the transmission coefficient without the load K_o into

$$K = K_o(1 + ZY)^{-1}.$$

The problem lies in the following: the load parameters, as, for example, input impedance of the next stage and parameters of the output impedance, heavily depend on the frequency of the signal. This does not allow to express K_u in its compact form. It is sufficient, if the components of output impedance and load conductivity are known:

$$Z(\omega) = r(\omega) + jx(\omega),$$

$$Y(\omega) = g(\omega) + jb(\omega).$$

At that, in the formation of output impedance Z, apart from IVD parameters, also parameters of commutational elements take part (Fig. 3). In order to calculate module K_u, one can use a simpler formula:

$$|K_u| \approx K_{uv}(1 - rg + xb).$$

Error component, caused by the reciprocal effect of two IVD stages, switched on in succession, having one commutational element between them, is shown in Fig. 1,b. It is necessary to note that there is a possibility of some error compensation from the load, selecting the deviation of active resistances (curve a).

Practical use of the proposed formulae makes it possible to quickly determine the error components in the IVD transmission coefficients of various configurations on the basis of simple impedance measurements of IVD circuits.

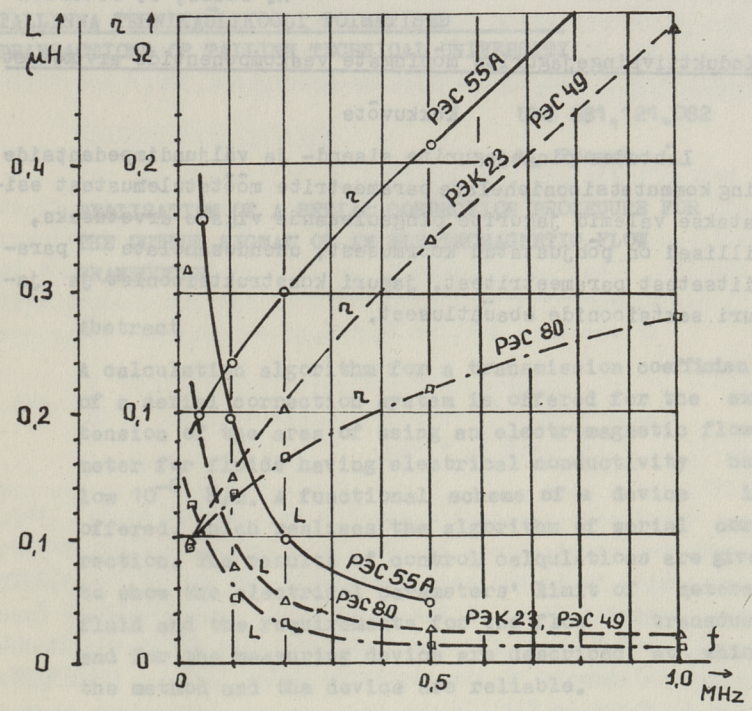

Fig. 3.

References

1. Baikov V.M. An analysis of errors in transformer voltage dividers // Proc. USSR Meteorological Institutes. 1968. Ed. 98/158. P. 125-143 (in Russian).

2. Bazilevich O.Z., Polischuk E.S. Errors of inductive voltage dividers and their identification // Precision-measuring Technique. Lvov. 1986. Ed. 39. P. 3-5 (in Russian).

R. Jõers, J. Peterson

Induktiivpingejagurite mõningate veakomponentide arvutusest

Kokkuvõte

Lähtudes pingejagurite sisend- ja väljundimpedantside ning kommutatsiooniahelate parameetrite mõõtetulemustest esitatakse valemid jagurite pingeülekande vigade arvutuseks, millised on põhjustatud koormusest, ühendusahelate parasiitsetest parameetritest, jaguri konstruktsioonist ja jaguri sektsioonide ebaühtlusest.

No 702

TALLINNA TEHNIKAÜLIKOOLI TOIMETISED
TRANSACTIONS OF TALLINN TECHNICAL UNIVERSITY

UDC 681.121.082

M. Toomet

REALISATION OF A SERIAL CORRECTION PROCEDURE FOR THE OUTPUT SIGNAL OF AN ELECTROMAGNETIC FLOW TRANSDUCER

Abstract

A calculation algorithm for a transmission coefficient of a serial correction system is offered for the extension of the area of using an electromagnetic flowmeter for fluids having electrical conductivity below 10^{-6} S/m. A functional scheme of a device is offered, which realises the algorithm of serial correction. The results of control calculations are given to show the electrical parameters' limit of metered fluid and the requirements for the flow transducer and for the measuring device are described, at which the method and the device are reliable.

Introduction

With the extension of the area of using an electromagnetic flowmeter to fluids having electrical conductivity below 10^{-6} S/m, a few problems arise, for instance the one of influencing the polarisation of metered fluid, which causes the decrease of the signal amplitude and the phase shift of the signal, generated by a flow transducer.

The perspective solution of the problem of influencing the polarisation of metered fluid, as considered by the author of the paper, is the method of a serial correction of the output signal of an electromagnetic flow transducer [1, 2].

As shown in [1], for the serial correction of the signal of an electromagnetic flow transducer, it is sufficient to determine the transmission coefficient for a

pilot signal, when the channel of the flow pipe is empty and when it is filled with metered fluid, while the frequency of the pilot signal is equal to that of the output signal of the transducer. The correction coefficient, to which the synphase signal component must be multiplied, is:

$$K_c = \frac{1}{1 - R_e\,(T_p/T_{po})}, \tag{1}$$

where

$$T_p = \frac{Y_p}{2\,Y_F + 2\,Y_{s1} + Y_p + Y_{s2}}, \tag{2}$$

$$T_{PO} = \frac{Y_p}{2\,Y_{s1} + Y_p + Y_{s2}}. \tag{3}$$

The synphase signal component is supposed to be the one of the output signal of the electromagnetic flow transducer, which is in the same phase with the one of the alternative magnetic field of the transducer. Conductivities Y_F, Y_{s1}, Y_p and Y_{s2} are complex conductivities of an electrical equivalent circuit of the electromagnetic flow tranducer, which is shown in Fig. 1.

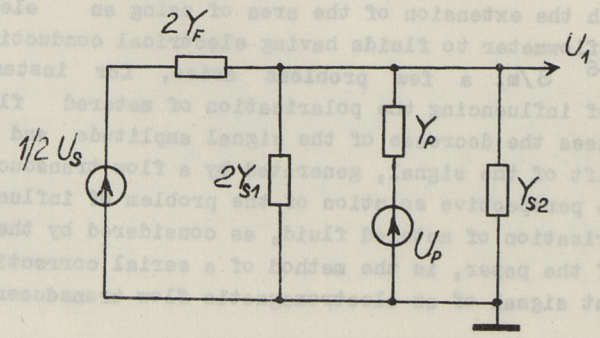

Fig. 1. The electrical equivalent circuit of the electromagnetic flow transducer.

Only half of the circuit is shown in Fig. 1, because the flow transducer has symmetrical configuration. U_s is the equivalent source of the output signal of the transducer and U_p is the equivalent source of the pilot signal.

Control Calculations

For the evaluation of the serial correction method realisation, control calculations are carried out. The results are represented in Table No 1. For the evaluation of the electrical equivalent circuit parameters of the flow transducer, the data and calculating formulas from [3] are used. The following signs are used in Table 1:

γ - electrical specific conductivity;
ε - relative dielectrical constant.

The values of the correction coefficient K_c and the transmission coefficients T_p and T_{po} have been calculated at the frequency of 500 Hz, using formulas (1), (2) and (3). The value of the frequency has been chosen as recommended in [3]. At the lines from 1 to 4 in Table 1, calculation results are represented, while the flow transducer is supposed to have surface electrodes. The value of the axial length of the electrodes was taken 10 mm. Serial correction method realisation requires that $Y \geq Y_F$, otherwise the value of T_p will become too small. (See line 4 to Table 1.)

The construction and technology of producing the flow transducer with surface electrodes are more complicated in comparison with the transducer with point electrodes, which are used in industrial production of electromagnetic flow transducers. Therefore, on line 5 in Table 1, calculation results are given in the case of point electrodes. As one can see from the results, serial correction method can be used up to the inner conductivity of flow transducer $\sigma_F \geq$ $\geq 10^{-10}$ S. The limit of using the electromagnetic flow transducer with point electrodes is determined by the value of the flow signal's transmission coefficient. The surface electrodes increase the transducer's inner conductivity and thus less conductive fluids flow rate can be measured.

Table 1

Results of Control Calculations

No	Y_f		Y_{s1}	Y_p	Y_{s2}		T_p	T_{p0}	K_c	Notes
	g_f (S)	C_f (pF)	C_{s1} (pF)	g_p (S)	g_{s2} (S)	C_{s2} (pF)				
1.	10^{-13}	0.2	0.1	10^{-9}	10^{-9}	0.1	0.171-j0.377	0.530-j0.499	2.11	$\gamma = 10^{-11}$ S/m; $\varepsilon = 2.2$
2.	10^{-10}	"	"	"	"	"	0.191-j0.350	"	2.09	$\gamma = 10^{-8}$ S/m; $\varepsilon = 2$
3.	10^{-9}	"	"	"	"	"	0.217-j0.158	"	1.58	$\gamma = 10^{-7}$ S/m; $\varepsilon = 2$
4.	10^{-8}	"	"	"	"	"	0.0471-j0.00493	"	1.05	$\gamma = 10^{-6}$ S/m; $\varepsilon = 2$
5.	10^{-10}	0.0002	0.0001	10^{-10}	10^{-10}	0.01	0.329-j0.0690	"	1.52	Point electrodes

Method Realization

It is suitable to use the voltage, which is generated in the coil, placed in the magnetic field of the electromagnetic flow transducer, as the pilot-signal. This pilot-signal may be switched on to the electrodes of the transducer by the calibrated conductivity Y_p. The selection of the transducer's output signal and the pilot signal may be done by summing and subtracting the voltages on the electrodes of the transducer, as shown in [2].

The realisation of the serial correction method of the electromagnetic flow transducer output signal requires the evaluation of the correction coefficient not by the parameters of the flow transducer's electrical equivalent circuit, but by the orthogonal components of the pilot signal on the output of the flow transducer.

For the expression of derivation (1) by the orthogonal components of the pilot signal, it is suitable to present (2) and (3) as follows:

$$T_P = \frac{U_{PS} + jU_{PQ}}{U_{PO}}, \tag{4}$$

$$T_{PO} = \frac{U'_{PS} + jU'_{PQ}}{U_{PO}}. \tag{5}$$

For the evaluation of the correction coefficient K_c by (1), it is necessary to determine the test signal transmission coefficient in the case of empty flow pipe and in the case of the pipe filled with the metered fluid. For this reason the following notions are introduced:

- the current value of the test signal at the output of the flow transducer; it means the voltage of the test signal in the case of the pipe filled with the metered fluid;
- the initial value of the voltage of the test signal in the case of empty flow pipe. In the formula (5), the components of the initial value of the test signal are indicated by an apostrophe. So in the formulas (4) and (5),

the following signs are used:

U'_{PO}, U_{PO} - the initial and the current values of the test signal,

U'_{PS}, U_{PS} - the initial and the current values of the synphase components of the test signal at the output of the flow transducer,

U'_{PQ}, U_{PQ} - the initial and the current values of the quadratic components of the test signal at the output of the flow transducer.

Thus, taking into account (4) and (5), it is possible to represent (1) as follows:

$$K_c = \frac{1}{1 - \frac{U'_{PO}\,(U'_{PS}\cdot U_{PS} + U'_{PQ}\cdot U_{PQ})}{U_{PO}\left[(U'_{PS})^2 + (U'_{PQ})^2\right]}}. \qquad (6)$$

The functional scheme of a device, which realizes the method of serial correction of the signal of the electromagnetic flow transducer, is represented in Fig. 2. The electrodes of the flow transducer 1 are connected with the calibrated conductivities Y_p and with voltage followers. The components of the flow transducer's output signal at the electrodes are in the opposite phase. The pilot signal at the electrodes are in the opposite phase. The pilot signal is switched on through the conductivities Y_p and has the same phase on both electrodes of the transducer. As mentioned above, the pilot signal is generated in the coil, placed in the magnetic field of the transducer. The outputs of the voltage followers are connected with the inputs of the differential and the summation amplifiers. The transducer's flow signal is selected from the mixture of the flow signal and the pilot signal at the output of the differential amplifier, because the components of the pilot signal compensate each other. At the output of the summation amplifier there is the voltage of the pilot signal, as the components of the flow signal compensate each other.

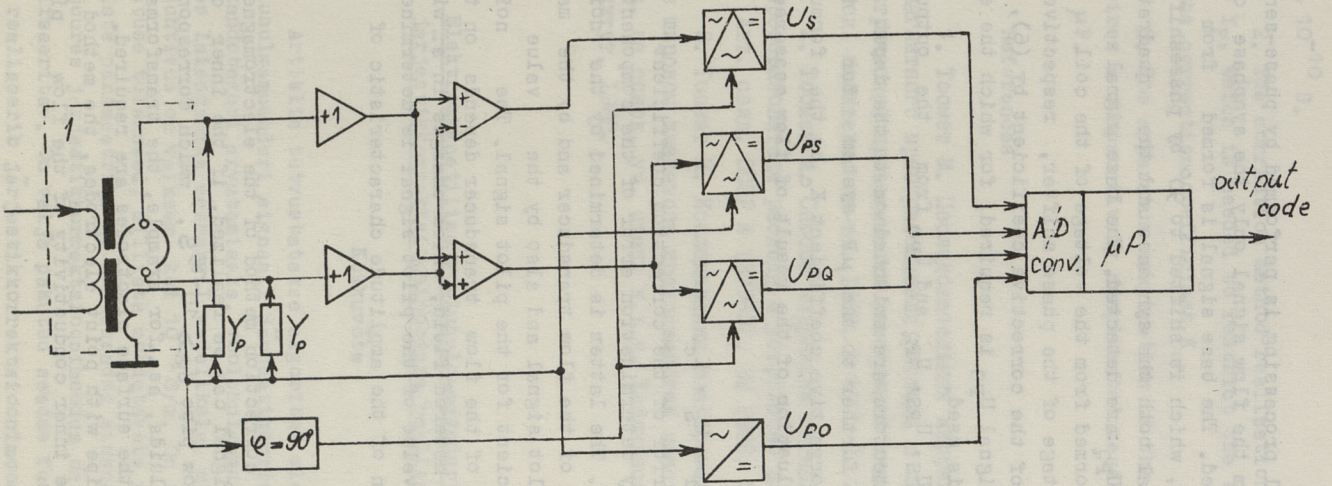

Fig. 2. The functional scheme of the electromagnetic flowmeter.

Further signal processing is performed by phase-sensitive detectors. From the flow signal only the synphase component U_S is detected. The base signal is formed from the voltage of the coil, which is shifted to 90° by phaseshifter. From the pilot signal both the synphase and the quadrature components U_{PS} and U_{PQ} are detected. The base signal for this procedure is formed from the voltage of the coil and from the output voltage of the phase shifter, respectively. For the evaluation of the corrective coefficient by (6), the value of the test signal U_{PO} is required, for which the expectation detector is used.

The voltages U_S, U_{PS}, U_{PQ} and U_{PO} from the outputs of corresponding detectors are switched on to the input of a A/D converter and further to the μP system for the evaluation of the corrective coefficient K_c by the formula (6) and for the evaluation of the result of flow measurement by the procedure

$$U_{OUT} = U_S \cdot K_c.$$

Calculation error of the correction coefficient by (6) is determined by determination error of the components of the pilot signal. The latter is determined by the noise level at the output of the flow transducer and by the maximum value of the pilot signal and also by the value of transmission coefficient for the pilot signal. The noise level at the output of the flow transducer depends on the conductivity of the metered fluid, which changes in a wide range. The maximum value of the pilot signal is determined by the linear region of the amplitude characteristic of the amplifiers.

Conclusions

1. The serial correction method of the electromagnetic flow transducer's signal can be realized, if the inner conductivity of the flow pipe $g_F \geq 10^{-13}$ S, which corresponds to the dielectric fluids, as, for example, the transformator oil. In this case, the surface electrodes are required. If one uses the flow pipe with point electrodes, the method will be suitable till the inner conductivity of the flow pipe

$g_F \geq 10^{-10}$ S.

2. The correction method realization requires that $Y_p \geq Y_F$, which is needed to restrict the evaluation error of the correction coefficient K_c.

3. The apparatus realization of the correction method requires a comparatively complicated measuring device with the μP.

References

1. Toomet M. Последовательная коррекция сигнала электромагнитного преобразователя расхода в широком диапазоне электрической проводимости измеряемой жидкости // Труды Таллиннск. политехн. ин-та. 1987. № 637. С. 36-41.

2. Toomet M. Способ коррекции сигнала электромагнитного преобразователя расхода и устройство для его осуществления. Авт. свид. СССР № 1379631, БИ 1988, № 9.

3. Toomet M. Исследование электромагнитного расходомера в широком диапазоне проводимостей измеряемой жидкости: Дисс. на соиск. уч. степ. к.т.н. Таллиннский политехнический институт, 1980.

M. Toomet

Elektromagnetilise vooluhulgamuunduri signaali järjestikkorrektsioonimooduse realiseerimine

Kokkuvõte

Artiklis tutvustatakse algoritmi elektromagnetilise vooluhulgamuunduri signaali järjestikkorrektsioonisüsteemi ülekandeteguri arvutamiseks, vooluhulgamuunduri kasutuspiirkonna laiendamise eesmärgil vedelikele, mille elektriline erijuhtivus on väiksem kui 10^{-6} S/m. On toodud kontrollarvutuse tulemused, milliste mõõdetavate vedelike elektriliste parameetrite ja mõõteseadme sisendahela parameetrite juures järjestikkorrektsioonimoodus on efektiivne ja realiseeritav. On välja pakutud seadme funktsionaalskeem, mis realiseerib järjestikkorrektsioonimooduse.

ТАЛЛИННСКИЙ ТЕХНИЧЕСКИЙ УНИВЕРСИТЕТ
ТРУДЫ ТТУ № 702
АНАЛИЗ И СИНТЕЗ СЛОЖНЫХ СИСТЕМ И ЦЕПЕЙ С ПОМОЩЬЮ ЭВМ
Электротехника и автоматика XXXУ111
На английском языке

Kogumiku on kinnitanud TTÜ Toimetiste kolleegium 15.12.89
Trükkida antud 15.12.89. Formaat 60x90/16
Trükipg. 4,25 + 0,25 (lisa). Arvestuspg. 3,7
Trükiarv 300. Tellimuse nr. 365/90
Hind 80 kop.
Tallinna Tehnikaülikool, 200108 Tallinn, Ehitajate tee 5
TTÜ rotaprint, 200006 Tallinn, Koskla 2/9

№ 702

TALLINNA TEHNIKAÜLIKOOLI TOIMETISED

ТРУДЫ ТАЛЛИННСКОГО ТЕХНИЧЕСКОГО УНИВЕРСИТЕТА

АНАЛИЗ И СИНТЕЗ СЛОЖНЫХ СИСТЕМ И ЦЕПЕЙ С ПОМОЩЬЮ ЭВМ

УДК 681.51

Формальная модель для автоматизированных технологических комплексов. Кулль А. - Труды Таллиннского технического университета. 1989. № 702. С. 3-10.

В статье рассматривается формальная модель для описания автоматизированных технологических комплексов. При моделировании автоматизированных технологических комплексов используется формализм дискретной событийной динамической системы. Рассматриваемая модель состоит из параллельно работающих процессов. Процессы взаимодействуют между собой через односторонние каналы связи. Процессы описываются с помощью расширенных конечных автоматов. Рассматриваемая формальная модель является достаточно универсальной для создания моделей различных систем управления реального времени.

Рисунков - 3, библ. наименований - 5.

УДК 681.514

Приближенное решение одномерной задачи оптимального сдвига с гауссовской функцией полезности и усеченным гауссовским распределением. Кийтам А. - Труды Таллиннского технического университета. 1989. № 702. С. 11-18.

Выведено уравнение для решения одномерной задачи сдвига с гауссовской функцией полезности и усеченным гауссовским распределением. Рассмотрены два приближенных решения для этого уравнения и их улучшение с помощью касательной.

Рисунков - 2, библ. наименований - 3.

УДК 681.514

Вычисление стохастических характеристик спектра выходного синусоидального сигнала цифро-аналогового преобразователя. Бахверк А. - Труды Таллиннского технического университета. 1989. № 702. С. 19-26.

Дано краткое описание двух возможностей генерирования синусоидального сигнала в виде дискретного периодического сигнала. В реальной ситуации генерируемый сигнал имеет случайные отклонения от заданной формы. Расчет стохастических характеристик спектра дискретного периодического сигнала проводится с помощью имитационного моделирования.

Рисунков - 7, библ. наименований - 3.

УДК 621.372.52 : 621.372.21

Характеристики выходной цепи с обратной связью, содержащей линию задержки. Кянгсеп Э. - Труды Таллиннского технического университета. 1989. № 702. С. 27-46.

Эта статья является попыткой нахождения (определения) физических ограничений для цепи с обратной связью, обусловленных временем распространения в проводах от источника до нагрузки. Приведены (найдены) теоретические выражения для выходной проводимости и переходной функции как для замкнутой, так и для разомкнутой цепи обратной связи. Приведены численные результаты для случая линии без потерь и идеального управляющего источника напряжения.

Рисунков - 10, библ. наименований - 2.

УДК 621.372.5

Общая волновая модель линейных во времени инвариантных четырехполюсников. Кянгсеп Э. - Труды Таллиннского технического университета. 1989. № 702, С. 47-52,

Эта статья является попыткой нахождения (определения) общей волновой модели для линейных во времени инвариантных четырехполюсников с целью использования ее при анализе во

временной области. Модель свертки для длинных линий, которая была представлена М. Валтоненым и использована другими авторами, является частным случаем здесь представленной модели.

Рисунков - 4, библ. наименований - 4.

УДК 621.317.727.1

Расчет компонент погрешностей передач напряжения трансформаторных делителей напряжения. Иыерс Р., Петерсон Я. - Труды Таллиннского технического университета. 1989. № 702. С. 53-58.

Рассматриваются вопросы расчета погрешностей коэффициента передачи напряжения трансформаторных делителей напряжения, обусловленные способом соединения обмоток, неравенством секции ступеней, нагрузкой, взаимным влиянием ступеней и коммутационными элементами. Предложены формулы для расчета этих погрешностей.

Рисунков - 3, библ. наименований - 2.

УДК 681.121.082

Осуществление последовательной коррекции сигнала электромагнитного преобразователя расхода. Тоомет М. - Труды Таллиннского технического университета. 1989. № 702. С. 59-68.

Предлагается вычислительный алгоритм для получения коэффициента передачи последовательной корректирующей системы с целью расширения диапазона применимости электромагнитного метода измерения расхода на жидкости, имеющие удельную электрическую проводимость ниже чем 10^{-6} См/м. Описывается функциональная схема устройства, которая реализует предлагаемый способ коррекций сигнала электромагнитного преобразователя расхода. Приводятся данные контрольного расчета, при каких электрических параметрах измеряемых жидкостей и преобразователя расхода, предлагаемые способы и устройство работоспособны.

Таблиц - 1, рисунков - 2, библ. наименований - 3.

Hind 80 kop.